A

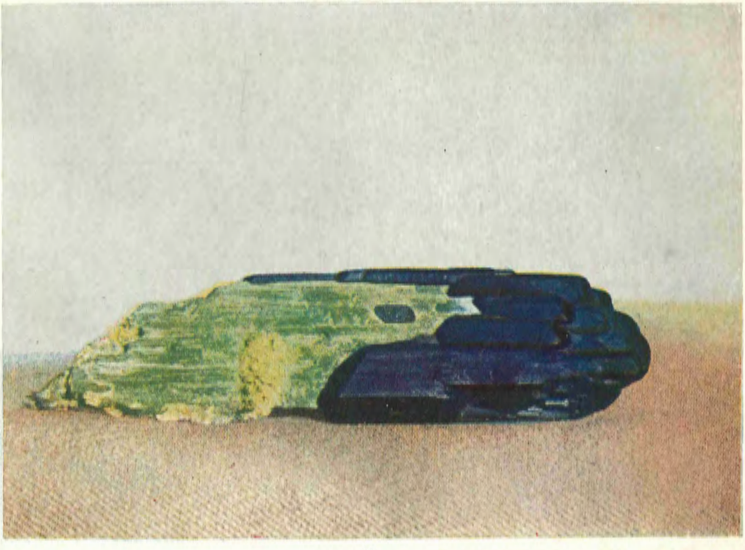

B

A. Three azurite crystals from Tsumeb, in parallel position, altering to malachite.

B. Pseudomorph of malachite after azurite from Bisbee, partially covered by second generation of azurite.

THE AMERICAN MINERALOGIST

JOURNAL OF THE MINERALOGICAL SOCIETY OF AMERICA

Vol. 12 APRIL, 1927 No. 4

CRYSTALLOGRAPHY OF AZURITE FROM TSUMEB, SOUTHWEST AFRICA, AND THE AXIAL RATIO OF AZURITE

CHARLES PALACHE AND LYMAN W. LEWIS.

CONTENTS

Explanation of Plates and Figures

Frontispiece.

A. Three azurite crystals from Tsumeb, in parallel position, altering to malachite. The concentric, radiating structure of the invading malachite fibers is well shown. The reproduction is natural size.

B. A large pseudomorph of malachite after azurite from Bisbee partially covered by a second generation of sub-parallel crystals of azurite. The later azurite is oriented parallel to the malachite pseudomorph. Natural size.

Explanation of Figures.

Figure 1. Azurite. Projections, in normal position, of crystal of type 1.

Figure 2, Pl. I. Azurite of type 1. Mag. 5 diam.

Figure 3. Orthographic and clinographic projections of azurite crystal, transitional between 1 and 2, due to the equal development of prism and front pinacoid.

Figure 4, Pl. I. Azurite transitional between types 1 and 2.

Figure 5, Pl. I. Crystal transitional between types 2 and 3. Mag. 2 diam.

Figure 6, Pl. I. Azurite of type 3. Mag. 5 diam.

Figure 7, Pl. II. Pseudo-rhombohedral aspect of one modification of type 4. Mag. 5 diam.

Figure 8, Pl. II. Simple modification dominated by base and unit prism.

Figure 9, Pl. II. Azurite of pyramidal habit. Mag. 5 diam.

Figure 10. Orthographic projection of a crystal of type 5.

Figure 11. Orthographic projection of a crystal of type 5 with important development of clinodomes and negative pyramids.

Figure 12, Pl. II. Azurite of type 6. Mag. 4 diam.

Figure 13, Pl. III. Azurite of type 7 with few forms. Mag. 5 diam.

Figure 14, Pl. III. Doubly terminated crystal of type 7. Mag. 10 diam.

Figure 15, Pl. III. Crystal of type 7 with complex terminations. Mag. 2 diam.

Figure 16, Pl. III. Crystal of type 7 dominated by the unit prism in the truncation.

Figure 17. Type 7. Orthographic projection on the side pinacoid, and clinographic projection in normal position, of crystal of azurite.

Figure 18. Type 7. Orthographic projection, on the side pinacoid, of azurite crystal, shown in figure 16.

Figure 19. Type 8. Orthographic projection, on the side pinacoid, of crystal shown in figure 20.

Figure 20, Pl. IV. Doubly terminated crystal of type 8 showing the prominent development of σ (101), *m* (110), *c* (001), and the clinodome zone.

Figure 21, Pl. IV. Simple representative of type 8 showing the typical striated appearance of the negative orthodome zone. Also the important development of λ ($\bar{2}$.18.3). Mag. 5 diam.

Figure 22, Pl. IV. Crystal tabular parallel to *c* (001) and μ ($\bar{1}05$), truncated by *m* (110). Mag. 5 diam.

Figure 23. Orthographic projection, on the side pinacoid, of a crystal of type 9, with *m* (110) the dominant truncation.

Figure 24. Orthographic projection, on the side pinacoid, of a crystal of type 9, with λ ($\bar{2}$.18.3) the dominant truncation.

Figure 25. Type 10. Orthographic projection, on the side pinacoid, and clinographic projection in normal position, of azurite crystal. This habit is very common in the collection, and includes the most perfect crystallographic material.

Figure 26, Pl. IV. Photograph illustrating the terminations of azurite shown in figure 25.

Figure 27. Type 10. Orthographic projection, on the side pinacoid, of a crystal of type 10. The modification is very striking where the flat pyramid λ ($\bar{2}$.18.3) forms the only important truncation.

Figure 28. Type 11. Orthographic and clinographic projections of a crystal of type 11. The symmetry of the ring of forms surrounding the base is not exaggerated.

Figure 29, Pl. IV. Crystal of type 12. It is interesting to compare this illustration with figures 5, 6 and 9 to note the change of habit resulting from variation in the relative development of *m* (110), *h* (221) *c* (001) and the clinodome zone.

Figure 30. Type 11. Orthographic and clinographic projections. The clinographic projection is turned 20° from the *b* axis to show more clearly the grouping of the faces at this end of the crystal.

Figure 31, Pl. V. Specimen containing unaltered azurite and completely malachitized azurite in contact.

Figure 32, Pl. V. Large azurite crystal of type 8 with bayldonite.

Figure 33. Orthographic and clinographic projections of a malachite pseudomorph of type 10 partially surrounded by a later azurite crystal of the same type in parallel position.

Figure 34, Pl. VI. Azurite altering to malachite.

Figure 35, Pl. VI. Pseudomorph group of malachite after azurite. The crystals are perfectly sharp, and the azurite forms can be positively identified. The color is lighter than many of the pseudomorphs, and on the velvety, apple-green faces the radiating structure is very conspicuous.

Figure 36, Pl. VII. Large pseudomorph of malachite after azurite. The sheaf-like structure of the malachite is well shown.

Figure 37, Pl. VII. Malachite pseudomorph after azurite. All the fibers on the front pinacoid radiate from one center. On the prism face there are many centers of radiation.

Figure 38. Orthographic projection, on the side pinacoid of an azurite crystal from Laurium, Greece, showing the new forms.

Figure 39. Clinographic projection and orthographic projection on the side pinacoid of azurite from Bisbee, Arizona, of the type shown on the pseudomorph in the color plate.

Figure 40. Gnomonic projection, on *b* (010), of all reported forms for azurite. In the negative orthodome zone no letter has been assigned to forms reported without one, but may be readily identified from the tables where the forms are listed in order of decreasing ϕ.

o New azurite forms.

● Azurite forms commonly observed on Tsumeb specimens.

. Other reported forms.

SUMMARY

It has repeatedly been asserted that the elements determined by Schrauf for azurite from Chessy, France, and used as the basis of calculated angles by Dana, Goldschmidt, and Groth are not in harmony with later measurements on specimens from other localities.

In the belief that the lack of agreement between measured and calculated angles was due to inferior crystals available for measurement by Schrauf, the present study was undertaken. New elements and angles have been calculated from measurements of many excellent crystals which furnish values more nearly in accord with observed angles. The material studied was chiefly a suite of minerals secured at the Tsumeb mine in 1922 by the senior author while a member of the Shaler Memorial Expedition to S. W. Africa. In this collection were over 1500 specimens containing crystallized azurite, or malachite pseudomorphs after azurite. Of this number 170 hand specimens of the most perfect or interesting types were chosen for careful study. Most of these were covered with brilliant, transparent azurite crystals well suited for crystallographic measurement.

METHODS

All the measurements were made on a Goldschmidt two-circle goniometer. Of the 28 crystals measured from Tsumeb, 15 were perfect enough to be used in the calculations, and had from 25 to 38 faces each. These were elongated parallel to the *b* axis and were measured with the orthodome zone parallel to the axis of the vertical circle. This allowed measurement of all the faces, (usually two of each form), of singly terminated crystals with one mounting. Only single, strong signals, observable with low magnification were considered of sufficient perfection to be used in computing the averages. The following table gives the weighted average, measured angles, in side pinacoid position, of the important faces.

A projection was made on the clinopinacoid, *b*(010), the symbols for this position were determined graphically, and the elements

Azurite Angle-Table Measured on (010) Used in Calculating Elements

Letter	Miller Symbol* 001	Miller Symbol* 010	Variation of ϕ ϕ to	ϕ	Average ϕ	Variation of ρ ρ to	ρ	Average ρ	Number of measurements used.
c	(001)	(100)	87°33′	87°37′	87°35′	89°57′	90°02′	90°00′	14
θ	$(\bar{1}01)$	$(\bar{1}10)$	$\overline{45}$ 07	$\overline{45}$ 14	$\overline{45}$ 11	89 57	90 01	"	8
v	$(\bar{2}01)$	$(\bar{1}20)$	$\overline{26}$ 06	$\overline{26}$ 35	$\overline{26}$ 22	89 58	90 00	"	12
η	$(\bar{3}02)$	$(\bar{2}30)$	$\overline{33}$ 06	$\overline{33}$ 48	$\overline{33}$ 30	90 00	90 01	"	9
σ	(101)	(110)	42 38	42 59	42 54	90 00	90 00	"	13
w	(120)	(012)	0 00	0 00	0 00	30 15	30 20	30 18	7
m	(110)	(011)	"	"	"	49 19	49 32	49 27	13
λ	$(\bar{2}.18.3)$	$(\bar{3}.2.18)$	$\overline{57}$ 04	$\overline{57}$ 24	$\overline{57}$ 15	12 40	12 44	12 41	10
R	$(\bar{2}41)$	$(\bar{1}24)$	$\overline{26}$ 10	$\overline{26}$ 20	$\overline{26}$ 17	32 32	32 34	32 33	11
k	$(\bar{2}21)$	$(\bar{1}22)$	$\overline{26}$ 13	$\overline{26}$ 20	$\overline{26}$ 17	51 54	51 58	51 56	13
h	(221)	(122)	25 19	25 26	25 23	52 50	52 58	52 52	12
s	(111)	(111)	42 54	42 57	42 55	58 55	58 58	58 57	5
P	(223)	(322)	53 48	53 58	53 52	64 31	64 39	64 34	9
γ	(121)	(112)	42 45	42 55	42 52	39 41	39 47	39 43	6
p	(021)	(102)	87 32	87 41	87 35	29 28	29 33	29 30	18
l	(023)	(302)	87 32	87 40	87 35	59 28	59 32	59 30	19
f	(011)	(101)	87 32	87 36	87 34	48 30	48 34	48 32	11

* $pqr(001) = rpq(010)$.

were then calculated according to the accepted practice.[1] From the averaged measured angles given in the above table the elements calculated on a representative number of faces is shown below:

[1] Charles Palache, *Am. Mineral.*, Vol. 5, No. 10, p. 177. The following formulas were used in the calculation and transformation:

$$x = \sin\phi \tan\rho = pp_0 \sin\mu$$

$$y = \cos\phi \tan\rho = qq_0 + pp_0 \cos\mu$$

$$\tan\mu = \frac{pp_0 \sin\mu}{pp_0 \cos\mu} = \frac{x}{y - pp_0}$$

$$p_0(001) = \frac{q_0}{p_0}(010) \qquad q_0(001) = \frac{1}{p_0}(010)$$

$$a = \frac{q_0}{p_0 \sin\mu} \qquad c = \frac{q_0}{\sin\mu}$$

Letter	Goldschmidt Symbol (010)	ϕ	ρ	pp_0''	p_0''	qq_0''	q_0''
R	$\bar{\frac{1}{4}}$ $\frac{1}{2}$	$\overline{26}$° 17′	32° 33′	.2829	1.1316	.5840	1.1680
k	$\bar{\frac{1}{2}}$ 1	$\overline{26}$ 17	51 56	.5659	1.1318	1.1688	1.1688
h	$\frac{1}{2}$ 1	25 23	52 52	.5666	1.1332	1.1692	1.1692
s	1	42 55	58 57	1.1320	1.1320	1.1689	1.1689
P	$\frac{3}{2}$ 1	53 52	64 34	1.7000	1.1322	1.1683	1.1683
p	$\frac{1}{2}$ 0	87 35	29 30	.5653	1.1306		
l	$\frac{3}{2}$ 0	87 35	59 30	1.6961	1.1307		
f	1 0	87 35	48 32	1.1306	1.1306		

μ(measured) = 87°35′. Average p_0'' = 1.1316. Average q_0'' = 1.1687. The measured value of μ was confirmed by calculation. Transformation to the normal position followed. (See footnote preceding).

$p_0 = 1.0326$. $q_0 = 0.8836$. $a = 0.8565$. $c = 0.8844$. $\beta = 87°35'$.

THE AXIAL RATIO OF AZURITE

Anderson[2] has pointed out the unsettled question regarding the values to be assigned to the elements of azurite. He publishes the following table to show "that Schrauf's elements, though correct no doubt for the azurite of Chessy, are not the best for crystals from other localities—."

Author	Locality	a	c	β
Schrauf	Chessy	.85012	.88054	87° 36′
Lacroix	"	.8469	.8789	87 39
Gonnard	"	.8477	.8792	.. ..
Farrington	Arizona	.85676	.88603	87 36 36″
Cohen	Broken Hill	.85608	.88585	87 38
Manasse	Calabonna	.85755	.88803	87 41
Anderson	Mineral Hill	.85721	.88581	87 34
To this list may be added:				
Toborffy	Tsumeb			87 38
Thomson	"	.8549	.8853	87 34
Aminoff	Bisbee	.8561	.8842	87 35
"	Broken Hill	.8563	.8850	87 41
Smith*	" "	.8565	.8850	87 36
Palache**	Bisbee, Broken Hill, Kelly, N. M.	.8568	.8841	87 36
Palache & Lewis	Tsumeb	.8564	.8844	87 35

* Unpublished notes.

** Weighted average from the three localities—unpublished notes.

[2] C. Anderson, *Jour. Proc. Roy. Soc. N. S. Wales*, Vol. LI.

This table shows that the Chessy values are materially smaller for both *a* and *c* than corresponding values derived from later studies, and that the elements presented in this paper are intermediate between the highest and lowest derived from other localities. This small difference in the elements is magnified to significant discrepancies in the calculated angles as illustrated in a comparison of the values for the unit prism:

$m \wedge m = 81° 06'$ Calculated from our elements.
$m \wedge m = 80° 41'$ Calculated from Schrauf's elements.

$\Delta = 0° 25'$

It was considered more desirable to base a new angle table on the elements derived from our study of the excellent Tsumeb crystals than on an average for all reported elements. Measurements subsequently made on crystals from other localities show very close agreement with our calculated angles, and indicate that the choice was justified. The confirmatory measurements are presented later in this paper.

The following angle table for all reported forms is based on the new elements. In the calculations Goldschmidt's formulas and system of checks were used, and the arrangement follows the system used in the Winkeltabellen.

AZURITE ANGLE TABLE FOR MEASUREMENTS ON THE BASE-(001)

$a=0.8565$	$\log a=9.93273$	$\log a_0=9.98608$
$c=0.8844$	$\log c=9.94665$	$\log b_0=0.05335$
$\left.\begin{matrix}\mu=\\180°\text{-}\beta\end{matrix}\right\}87°\ 35'$	$\left.\begin{matrix}\log h=\\\log\sin\mu\end{matrix}\right\}9.99961$	$\left.\begin{matrix}\log e=\\\log\cos\mu\end{matrix}\right\}8.62497$
$\log p_0=0.01396$	$a_0=0.9684$	$p_0=1.0326$
$\log q_0=9.94627$	$b_0=1.1307$	$q_0=0.8836$
$\log\frac{q_0}{p_0}=0.06769$	$h=0.9998$	$e=0.0422$

Number	Letter	Miller Symbol (001)	ϕ	ρ	ξ_0	η_0	ξ	η	x'	y'	d'
1	*c*	001	90°00′	2°25′	2°25′	0°00′	2°25′	0°00′		0	
2	*b*	010	0 00	90 00	0 00	90 00	0 00	90 00	0	∞	∞
3	*a*	100	90 00	"	90 00	0 00	90 00	0 00	∞	0	"
4	*u*	310	74 05	"	"	90 00	74 05	15 55		∞	"
5	*g*	210	66 50	"	"	90 00	66 50	23 10		"	"
6	*i*	320	60 18	"	"	"	60 18	29 42		"	"
7	*m*	110	49 27	"	"	"	49 27	40 33		"	"
8	*w*	120	30 18	"	"	"	30 18	59 42		"	"
9	*e*	0.1.10	25 31	5 36	2 25	5 03	2 24	5 03	0.0422	0.0884	0.0980
10	*C*	018	20 54	6 45	2 25	6 19	2 24	6 18	0.0422	0.1106	0.1183
11	*G*	016	15 59	8 43	"	8 23	2 23	8 22	"	0.1474	0.1533
12	Λ	015	13 25	10 18	"	10 02	2 23	10 01	"	0.1769	0.1818
13	*S*	014	10 48	12 41	"	12 28	2 22	12 27	"	0.2211	0.2251
14		027	7 33	17 47	"	17 59	2 18	17 38	"	0.3181	0.3209
15	*q*	025	6 47	19 36	"	19 29	2 17	19 28	"	0.3538	0.3563
16	*E*	012	5 27	23 57	"	23 51	2 13	23 50	"	0.4422	0.4442
17	*l*	023	4 05	30 35	"	30 32	2 05	30 30	"	0.6033	0.5911
18	𝔑	034	3 38	33 37	"	33 34	2 01	33 32	"	0.6610	0.6647
19	*j*	045	3 25	34 05	"	35 17	2 00	35 52	"	0.7075	0.6769
20	*f*	011	2 44	41 31	"	41 29	1 49	41 27	"	0.8844	0.8854
21		076	2 20	45 55	"	45 54	1 41	45 53	"	1.0318	1.0327
22	*K*	032	1 49	53 00	"	53 00	1 27	52 58	"	1.3266	1.3273
23	*p*	021	1 22	60 32	"	60 31	1 11	60 30	"	1.7688	1.7693
24	*L*	031	0 55	69 21	"	69 21	0 51	69 19	"	2.6532	2.6536
25	Ω	301	90 00	72 21	72 21	0 00	72 21	0 00	3.1428	0	3.1428
26	ϕ	201	90 00	64 38	64 38	0 00	64 38	0 00	2.1093	"	2.1093

Number	Letter	Miller Symbol (001)	ϕ	ρ	ξ_0	η_0	ξ	η	x'	y'	d'
27		905	90°00′	62°17′	62°17′	0°00′	62°17′	0°00′	1.9026	0	1.9026
28	σ	101	"	47 06	47 06	"	47 06	"	1.0758	"	1.0758
29	ℌ	203	"	36 11	36 11	"	36 11	"	0.7313	"	0.7313
30	ζ	102	"	29 13	29 13	"	29 13	"	0.5590	"	0.5590
31	𝔯	307	"	25 53	25 53	"	25 53	"	0.4852	"	0.4852
32		205	"	24 30	24 30	"	24 30	"	0.4556	"	0.4556
33	*M*	104	"	16 44	16 44	"	16 44	"	0.3006	"	0.3006
34	*r*	$\bar{1}08$	90 00	4 58	$\bar{4}$ 58	0 00	$\bar{4}$ 58	0 00	$\bar{0}.0870$	0	0.0870
35		$\bar{1}07$	"	6 01	$\bar{6}$ 01	"	$\bar{6}$ 01	"	$\bar{0}.1054$	"	0.1054
36		$\bar{1}06$	"	7 24	$\bar{7}$ 24	"	$\bar{7}$ 24	"	$\bar{0}.1300$	"	0.1300
37		$\bar{2}.0.11$	"	8 17	$\bar{8}$ 17	"	$\bar{8}$ 17	"	$\bar{0}.1456$	"	0.1456
38	μ	$\bar{1}05$	"	9 21	$\bar{9}$ 21	"	$\bar{9}$ 21	"	$\bar{0}.1645$	"	0.1645
39		$\bar{4}.0.19$	"	9 57	$\bar{9}$ 57	"	$\bar{9}$ 57	"	$\bar{0}.1754$	"	0.1754
40		$\bar{3}.0.14$	"	10 10	$\overline{10}$ 10	"	$\overline{10}$ 10	"	$\bar{0}.1793$	"	0.1793
41	*D*	$\bar{1}04$	"	12 12	$\overline{12}$ 12	"	$\overline{12}$ 12	"	$\bar{0}.2162$	"	0.2162
42	*F*	$\bar{2}07$	"	14 12	$\overline{14}$ 12	"	$\overline{14}$ 12	"	$\bar{0}.2531$	"	0.2531
43		$\bar{3}.0.10$	"	15 00	$\overline{15}$ 00	"	$\overline{15}$ 00	"	$\bar{0}.2678$	"	0.2678
44		$\bar{4}.0.13$	"	16 01	$\overline{16}$ 01	"	$\overline{16}$ 01	"	$\bar{0}.2758$	"	0.2758
45	*A*	$\bar{1}03$	"	16 49	$\overline{16}$ 49	"	$\overline{16}$ 49	"	$\bar{0}.3023$	"	0.3023
46		$\bar{4}.0.11$	"	18 27	$\overline{18}$ 27	"	$\overline{18}$ 27	"	$\bar{0}.3336$	"	0.3336
47	*J*	$\bar{2}05$	"	20 22	$\overline{20}$ 22	"	$\overline{20}$ 22	"	$\bar{0}.3712$	"	0.3712
48	*n*	$\bar{1}02$	"	25 23	$\overline{25}$ 23	"	$\overline{25}$ 23	"	$\bar{0}.4745$	"	0.4745
49		$\bar{2}03$	"	32 54	$\overline{32}$ 54	"	$\overline{32}$ 54	"	$\bar{0}.6468$	"	0.6468
50	*N*	$\bar{5}07$	"	34 50	$\overline{34}$ 50	"	$\overline{34}$ 50	"	$\bar{0}.6959$	"	0.6959
51	*T*	$\bar{4}05$	"	38 07	$\overline{38}$ 07	"	$\overline{38}$ 07	"	$\bar{0}.7846$	"	0.7846
52		$\overline{11}.0.13$	"	39 46	$\overline{39}$ 46	"	$\overline{39}$ 46	"	$\bar{0}.8322$	"	0.8322
53	θ	$\bar{1}01$	"	44 45	$\overline{44}$ 45	"	$\overline{44}$ 45	"	$\bar{0}.9913$	"	0.9913
54	𝔓	$\bar{9}08$	"	48 15	$\overline{48}$ 15	"	$\overline{48}$ 15	"	$\bar{1}.1203$	"	1.1203
55	*W*	$\bar{6}05$	"	50 09	$\overline{50}$ 09	"	$\overline{50}$ 09	"	$\bar{1}.1970$	"	1.1970
56	*B*	$\bar{5}04$	"	51 16	$\overline{51}$ 16	"	$\overline{51}$ 06	"	$\bar{1}.2470$	"	1.2470
57	κ	$\bar{4}03$	"	53 11	$\overline{53}$ 11	"	$\overline{53}$ 11	"	$\bar{1}.3358$	"	1.3358
58	η	$\bar{3}02$	"	56 24	$\overline{56}$ 24	"	$\overline{56}$ 24	"	$\bar{1}.5045$	"	1.5045
59		$\bar{5}03$	"	59 15	$\overline{59}$ 15	"	$\overline{59}$ 15	"	$\bar{1}.6803$	"	1.6803
60	𝔉	$\bar{7}04$	"	60 29	$\overline{60}$ 29	"	$\overline{60}$ 29	"	$\bar{1}.7664$	"	1.7664
61		$\overline{15}.0.8$	"	62 11	$\overline{62}$ 11	"	$\overline{62}$ 11	"	$\bar{1}.8956$	"	1.8956
62	*v*	$\bar{2}01$	"	63 43	$\overline{63}$ 43	"	$\overline{63}$ 43	"	$\bar{2}.0249$	"	2.0249
63	𝔐	$\overline{13}.0.6$	"	65 32	$\overline{65}$ 32	"	$\overline{65}$ 32	"	$\bar{2}.1980$	"	2.1980
64	𝔛	$\bar{7}03$	"	67 07	67 07	"	67 07	"	$\bar{2}.3694$	"	2.3694
65		$\overline{19}.0.8$	"	67 30	$\overline{67}$ 30	"	$\overline{67}$ 30	"	$\bar{2}.4128$	"	2.4128
66	ψ	$\bar{3}01$	"	71 54	$\overline{71}$ 54	"	$\overline{71}$ 54	"	$\bar{3}.0585$	"	3.0585
67		$\bar{7}02$	"	74 23	$\overline{74}$ 23	"	$\overline{74}$ 23	"	$\bar{3}.5751$	"	3.5751
68	*h*	221	50 01	70 02	64 38	60 31	46 04	37 09	2.1091	1.7682	2.7526
69	*s*	111	50 35	54 19	47 05	41 29	38 46	31 03	1.0757	0.8844	1.3925

Number	Letter	Miller Symbol (001)	ϕ	ρ	ξ_0	η_0	ξ	η	x'	y'	d'
70	P	223	51°07′	43°12′	36°10′	30°32′	32°12′	25°27′	0.7313	0.5896	0.9394
71	$\mathfrak{p}$	112	51 39	35 28	29 12	23 51	27 05	21 06	0.5590	0.4422	0.7128
72	t	$\bar{2}25$	$\overline{46}$ 22	27 09	$\overline{20}$ 21	19 29	$\overline{19}$ 17	17 55	$\bar{0}$.3711	0.3538	0.5127
73	Q	$\bar{1}12$	$\overline{46}$ 53	32 54	$\overline{25}$ 17	23 51	$\overline{23}$ 22	21 48	$\bar{0}$.4724	0.4422	0.6471
74	z	$\bar{4}47$	$\overline{47}$ 16	36 45	$\overline{28}$ 44	26 49	$\overline{26}$ 04	23 57	$\bar{0}$.5484	0.5054	0.7465
75	u	$\bar{2}23$	$\overline{47}$ 39	41 11	$\overline{32}$ 54	30 31	$\overline{29}$ 08	26 20	$\bar{0}$.6468	0.5896	0.8752
76	x	$\bar{1}11$	$\overline{48}$ 16	53 02	$\overline{44}$ 45	41 29	$\overline{36}$ 36	32 08	$\bar{0}$.9913	0.8844	1.3284
77	k	$\bar{2}21$	$\overline{48}$ 52	69 36	$\overline{63}$ 43	60 31	$\overline{44}$ 54	38 04	$\bar{2}$.0242	1.7682	2.6822
78	π	$\bar{4}41$	$\overline{49}$ 20	79 32	$\overline{76}$ 15	74 13	$\overline{47}$ 58	39 56	$\bar{4}$.1763	3.5376	5.4370
79	$\mathfrak{C}$	$\bar{7}71$	$\overline{49}$ 17	83 59	$\overline{82}$ 05	80 49	$\overline{48}$ 55	40 27	7.1926	6.1910	9.4903
80	$\mathfrak{q}$	212	67 39	49 19	47 05	23 51	26 16	16 45	0 1076	0.4422	1.1631
81	γ	121	31 18	64 14	47 05	60 28	27 53	50 18	1.0757	1.7682	2.0710
82	Σ	$\bar{2}32$	$\overline{36}$ 46	58 53	$\overline{44}$ 45	52 59	$\overline{30}$ 49	43 18	$\bar{0}$.9913	1.3264	1.6947
83	ν	$\bar{3}53$	$\overline{33}$ 56	60 37	$\overline{44}$ 45	55 50	$\overline{29}$ 02	46 18	$\bar{0}$.9913	1.4735	1.7758
84	α	$\bar{1}21$	$\overline{29}$ 16	63 45	$\overline{44}$ 45	60 31	$\overline{26}$ 00	51 29	$\bar{0}$.9913	1.7682	2.0277
85	$\mathfrak{m}$	525	70 23	46 25	44 45	19 29	43 02	14 05	0.9913	0.3537	1.0509
86	$\mathfrak{e}$	131	20 29	70 33	44 45	69 21	19 16	62 03	0.9913	2.6533	2.8324
87	$\mathfrak{r}$	122	32 18	46 18	29 12	41 30	31 28	31 26	0.5590	0.8844	1.0463
88		$\bar{3}22$	$\overline{59}$ 37	60 14	$\overline{56}$ 27	41 29	$\overline{48}$ 29	26 03	$\bar{1}$.5081	0.8844	1.7482
89	y	$\bar{2}11$	$\overline{66}$ 24	65 39	$\overline{63}$ 43	41 29	$\overline{56}$ 35	21 24	$\bar{2}$.0242	0.8844	2.2096
90	z	$\bar{4}11$	$\overline{77}$ 46	76 32	$\overline{76}$ 14	41 29	$\overline{71}$ 52	11 54	$\bar{4}$.0816	0.8844	4.1764
91	ω	241	30 48	76 21	64 38	74 13	29 50	56 35	2.1091	3.5380	4.1193
92	$\mathfrak{t}$	$\bar{6}83$	$\overline{40}$ 39	72 10	$\overline{63}$ 43	67 01	$\overline{38}$ 19	46 14	$\bar{2}$.0242	2.3580	3.1083
93	R	$\overline{24}1$	$\overline{29}$ 47	76 13	$\overline{63}$ 43	74 13	$\overline{28}$ 54	57 27	$\bar{2}$.0242	3.5380	4.0764
94	t	$\bar{2}61$	$\overline{20}$ 53	80 02	$\overline{63}$ 43	79 20	$\overline{20}$ 33	66 57	$\bar{2}$.0242	5.3065	5.6796
95	τ	$\bar{4}72$	$\overline{33}$ 11	74 52	$\overline{63}$ 43	72 06	$\overline{31}$ 54	53 53	$\bar{2}$.0248	3.0955	3.6989
96	$\mathfrak{h}$	$\bar{2}$.10.1	$\overline{13}$ 25	83 43	$\overline{64}$ 38	83 33	$\overline{13}$ 01	75 13	$\bar{2}$.1093	8.8443	9.0922
97	ξ	321	60 38	74 30	72 21	60 31	57 07	28 34	3.1428	1.7682	2.6061
98	G	$\bar{3}21$	$\overline{59}$ 57	74 12	$\overline{71}$ 53	60 31	$\overline{56}$ 24	28 48	$\bar{3}$.0583	1.7682	3.5333
99	$\mathfrak{u}$	$\bar{3}51$	$\overline{34}$ 40	79 28	$\overline{71}$ 54	77 15	$\overline{34}$ 00	53 57	$\bar{3}$.0584	4.4221	5.3767
100	$\mathfrak{i}$	$\bar{6}81$	$\overline{41}$ 02	83 55	$\overline{80}$ 47	82 47	$\overline{40}$ 46	48 35	$\bar{6}$.1589	7.0754	9.3806
101	$\mathfrak{d}$	$\bar{4}$.10.1	$\overline{24}$ 50	84 08	$\overline{76}$ 16	83 33	$\overline{24}$ 41	64 32	$\bar{4}$.0919	8.8443	9.7450
102	$\mathfrak{f}$	6.10.1	35 13	84 43	80 54	83 33	35 03	54 26	6.2434	8.8443	10.8260
103	K	$\overline{12}$.10.5	$\overline{54}$ 03	71 38	$\overline{67}$ 42	60 31	$\overline{50}$ 12	35 52	$\bar{2}$.4382	1.7682	3.0123
104	J	132	22 51	55 13	29 12	53 00	18 36	49 11	0.5590	1.3266	1.4396
105	χ	1.11.2	6 33	78 28	29 12	78 23	6 25	76 45	0.5590	4.8642	4.8961
106	i	$\bar{1}$.10.2	$\bar{6}$ 07	77 20	$\overline{25}$ 23	77 15	$\bar{5}$ 59	75 57	$\bar{0}$.4745	4.4221	4.4474
107	β	$\bar{3}62$	$\overline{29}$ 37	71 52	$\overline{56}$ 27	69 21	$\overline{28}$ 01	55 42	$\bar{1}$.5080	2.6532	0.3052
108	T	4.12.3	21 52	75 18	54 52	74 13	21 07	63 51	1.4203	3.5377	3.8122
109	ρ	$\bar{1}34$	$\overline{18}$ 17	34 35	$\overline{12}$ 12	33 12	$\overline{10}$ 15	32 36	$\bar{0}$.2161	0.6545	0.6892
110	$\mathfrak{b}$	$\bar{5}28$	$\overline{69}$ 53	32 44	$\overline{31}$ 07	12 28	$\overline{30}$ 31	10 43	$\bar{0}$.6037	0.2211	0.6429
111	S	$\bar{1}25$	$\overline{24}$ 53	21 19	$\bar{9}$ 19	19 27	$\bar{8}$ 48	19 15	$\bar{0}$.1641	0.3538	0.3900
112	λ	$\bar{2}$.18.3	$\bar{6}$ 57	79 24	$\overline{32}$ 54	79 20	$\bar{6}$ 50	77 21	$\bar{0}$.6468	5.3064	5.3451

Number	Letter	Miller Symbol (001)	ϕ	ρ	ξ_0	η_0	ξ	η	x'	y'	d'
113	δ	243	31°42′	54°11′	36°03′	49°42′	25°13′	47°38′	0.7279	1.1789	1.3855
114	*d*	$\bar{2}43$	$\bar{28}$ 45	53 22	$\bar{32}$ 54	49 42	$\bar{22}$ 42	44 43	$\bar{0}.6468$	1.1789	1.3447
115	Δ	$\bar{2}.10.3$	$\bar{12}$ 23	71 40	$\bar{32}$ 54	71 16	$\bar{11}$ 44	68 00	$\bar{0}.6468$	2.9478	3.0179
116	𝔡	9.12.8	42 15	60 50	50 18	53 00	35 57	40 16	1.2049	1.3266	1.7919
117	*e*	$\bar{2}45$	$\bar{27}$ 41	38 38	$\bar{20}$ 22	35 17	$\bar{16}$ 52	33 34	$\bar{0}.3712$	0.7075	0.7990
118	*H*	4.10.7	26 36	54 43	32 20	51 38	21 26	46 52	0.6328	1.2634	1.4131
119	*o*	685	42 11	62 22	52 03	54 45	36 30	41 02	1.2825	1.4151	1.9097
120	𝔤	283	17 13	67 57	36 40	67 01	15 56	62 17	0.7312	2.3585	2.4693
121	Φ	$\bar{2}73$	$\bar{17}$ 24	65 11	$\bar{32}$ 54	64 09	$\bar{15}$ 45	60 40	$\bar{0}.6468$	2.0637	2.1627
122	𝔧	$\bar{4}76$	$\bar{32}$ 05	50 36	$\bar{32}$ 54	45 54	$\bar{24}$ 14	40 54	$\bar{0}.6468$	1.0319	1.2178
123	𝔣	153	14 42	56 44	21 09	55 51	12 15	53 58	0.3867	1.4741	1.5240
124	𝔩	$\bar{7}43$	$\bar{63}$ 32	69 18	$\bar{67}$ 07	49 42	$\bar{56}$ 50	24 38	$\bar{2}.3694$	1.1793	2.6465
125	𝔷	287	18 28	46 49	18 39	45 18	13 21	43 46	0.3375	1.0108	1.0657
126	𝔯	$\bar{5}73$	$\bar{39}$ 09	69 24	$\bar{59}$ 14	64 09	$\bar{36}$ 14	46 33	$\bar{1}.6803$	2.0637	2.6613
127	𝔖	245	32 58	40 09	24 39	35 17	20 32	32 45	0.4589	0.7075	0.8434
128	𝔘	564	45 10	62 01	53 09	52 59	38 46	38 31	1.3341	1.3266	1.8814
129	𝔇	453	43 56	63 58	54 51	55 51	38 34	40 19	1.4203	1.4741	2.0468
130	𝔫	231	38 29	73 34	64 38	69 20	36 39	48 40	2.1093	2.6533	3.3896

As azurite is commonly enlongated parallel to the *b* axis, it is often desirable to measure crystals with the orthodome zone prismatic. The following table gives the calculated angles for this position. The numbering and arrangement follows the first table to lessen confusion between the two positions.

The transformation of angles and symbols is effected by use of the relationship:

$$\phi\ (010) = 90 - \xi_0(001)$$
$$\rho\ (010) = 90 - \eta(001)$$
$$pqr\ (001) = rpq(010)$$

Azurite Angle Table for Measurements on the Side Pinacoid-(010)

$p_0''=1.1316$	$q_0''=1.1687$	$\mu=87° 35'$

Number	Letter	Miller Symbol (010)	Miller Symbol (001)	ϕ	ρ
1	*c*	100	001	87° 35′	90° 00′
2	*b*	001	010	0 00	0 00
3	*a*	010	100	0 00	90 00
4	*u*	031	310	0 00	74 05
5	*g*	021	210	0 00	66 50
6	*i*	032	320	0 00	60 18
7	*m*	011	110	0 00	49 27
8	*w*	012	120	0 00	30 18
9	*e*	10.0.1	0.1.10	87 35	84 57
10	*C*	801	018	"	83 42
11	*G*	601	016	"	81 38
12	Λ	501	015	"	79 59
13	*S*	401	014	"	77 33
14		702	027	"	72 22
15	*q*	502	025	"	70 32
16	*E*	201	012	"	66 10
17	*l*	302	023	"	59 30
18	ℜ	403	034	"	56 28
19	*j*	504	045	"	54 08
20	*f*	101	011	"	48 33
21		607	076	"	44 07
22	*K*	203	032	"	37 02
23	*p*	102	021	"	29 30
24	*L*	103	031	"	20 41
25	Ω	130	301	17 39	90 00
26	ϕ	120	201	25 22	"
27		590	905	27 43	"
28	σ	110	101	42 54	"
29	ℌ	320	203	53 49	"
30	ζ	210	102	60 47	"
31	𝔯	730	307	64 07	"
32		520	205	65 30	"
33	*M*	410	104	73 16	"
34	*r*	$\bar{8}10$	$\bar{1}08$	$\overline{85}$ 02	"
35		$\bar{7}10$	$\bar{1}07$	$\overline{83}$ 59	"
36		$\bar{6}10$	$\bar{1}06$	$\overline{82}$ 36	"
37		$\overline{11}.2.0$	$\bar{2}.0.11$	$\overline{81}$ 43	"
33	μ	$\bar{5}10$	$\bar{1}05$	$\overline{80}$ 39	"
89		$\overline{19}.4.0.$	$\bar{4}.0.19$	$\overline{80}$ 03	"

Number	Letter	Miller Symbol	Miller Symbol	ϕ	σ
40		$\overline{14}.3.0$	$\bar{3}.0.14$	$\overline{79}$° 50′	90° 00′
41	*D*	$\bar{4}10$	$\bar{1}04$	$\overline{77}$ 48	"
42	*F*	$\bar{7}20$	$\bar{2}07$	$\overline{75}$ 48	"
43		$\overline{10}.3.0.$	$\bar{3}.0.10$	$\overline{75}$ 00	"
44		$\overline{13}.4.0$	$\bar{4}.0.13$	$\overline{73}$ 59	"
45	*A*	$\bar{3}10$	$\bar{1}03$	$\overline{73}$ 11	"
46		$\overline{11}.4.0$	$\bar{4}.0.11$	$\overline{71}$ 33	"
47	*J*	$\bar{5}20$	$\bar{2}05$	$\overline{69}$ 38	"
48	*n*	$\bar{2}10$	$\bar{1}02$	$\overline{64}$ 37	"
49		$\bar{3}20$	$\bar{2}03$	$\overline{57}$ 06	"
50	*N*	$\bar{7}50$	$\bar{5}07$	$\overline{55}$ 10	"
51	*T*	$\bar{5}40$	$\bar{4}05$	$\overline{51}$ 53	"
52		$\overline{13}.11.0$	$\overline{11}.0.13$	$\overline{50}$ 14	"
53	θ	$\bar{1}10$	$\bar{1}01$	$\overline{45}$ 15	"
54	𝔓	$\bar{8}90$	$\bar{9}08$	$\overline{41}$ 45	"
55	*W*	$\bar{6}50$	$\bar{6}05$	$\overline{39}$ 51	"
56	*B*	$\bar{4}50$	$\bar{5}04$	$\overline{38}$ 44	"
57	κ	$\bar{3}40$	$\bar{4}03$	$\overline{36}$ 49	"
58	η	$\bar{2}30$	$\bar{3}02$	$\overline{33}$ 36	"
59		$\bar{3}50$	$\bar{5}03$	$\overline{30}$ 45	"
60	𝔉	$\bar{4}70$	$\bar{7}04$	$\overline{29}$ 31	"
61		$\bar{8}.15.0$	$\overline{15}.0.8$	$\overline{27}$ 49	"
62	*v*	$\bar{1}20$	$\bar{2}01$	$\overline{26}$ 17	"
63	𝔐	$\bar{6};13;0$	$\overline{13};0;6$	$\overline{24}$ 28	"
64	𝔛	$\bar{3}70$	$\bar{7}03$	$\overline{22}$ 53	"
65		$\bar{8}.19.0$	$\overline{19}.0.8$	$\overline{22}$ 30	"
66	ψ	$\bar{1}30$	$\bar{3}01$	$\overline{18}$ 06	"
67		$\bar{2}70$	$\bar{7}02$	$\overline{15}$ 37	"
68	*h*	122	221	25 22	52 51
69	*s*	111	111	42 55	58 57
70	*P*	322	223	53 50	64 33
71	𝔭	211	112	60 48	68 54
72	*t*	$\bar{5}22$	$\bar{2}25$	$\overline{69}$ 39	72 05
73	*Q*	$\bar{2}11$	$\bar{1}12$	$\overline{64}$ 43	68 12
74	*z*	$\bar{7}44$	$\bar{4}47$	$\overline{61}$ 16	66 03
75	*u*	$\bar{3}22$	$\bar{2}23$	$\overline{57}$° 06′	$\overline{63}$° 40′
76	*x*	$\bar{1}11$	$\bar{1}11$	$\overline{45}$ 15	57 52
77	*k*	$\bar{1}22$	$\bar{2}21$	$\overline{26}$ 17	51 56
78	π	$\bar{1}44$	$\bar{4}41$	$\overline{13}$ 45	50 04
79	ℭ	$\bar{1}77$	$\bar{7}71$	$\bar{7}$ 55	49 33
80	𝔮	221	212	42 55	73 15
81	γ	112	121	42 55	39 42
82	Σ	$\bar{2}23$	$\bar{2}32$	$\overline{45}$ 15	46 42
83	ν	$\bar{3}35$	$\bar{3}53$	"	43 42
84	α	$\bar{1}12$	$\bar{1}21$	"	38 31

Number	Letter	Miller Symbol (010)	Miller Symbol (001)	ϕ	ρ
85	𝔴	$\bar{5}52$	$\bar{5}25$	$\overline{45}$° 15′	75° 55′
86	𝔢	$\bar{1}13$	$\bar{1}31$	"	27 57
87	𝔯	212	122	60 48	58 34
88		232	322	33 33	65 57
89	*y*	$\bar{1}21$	$\bar{2}11$	$\overline{26}$ 17	68 36
90	*z*	$\bar{1}41$	$\bar{4}11$	$\overline{13}$ 46	78 06
91	*ω*	124	241	25 22	33 25
92	*τ*	$\bar{3}68$	$\bar{6}83$	$\overline{26}$ 17	45 46
93	*R*	$\bar{1}24$	$\bar{2}41$	"	32 33
94	*t*	$\bar{1}26$	$\bar{2}61$	"	23 03
95	𝔱	$\bar{2}47$	$\bar{4}72$	"	36 05
96	𝔥	$\bar{1}$.2.10	$\bar{2}$.10.1	"	14 09
97	*ξ*	132	321	17 39	61 26
98	*G*	$\bar{1}32$	$\bar{3}21$	$\overline{18}$ 07	61 12
99	𝔲	$\bar{1}35$	$\bar{3}51$	"	36 03
100	𝔦	$\bar{1}68$	$\bar{6}81$	$\bar{9}$ 13	41 25
101	𝔬	$\bar{1}$.4.10	$\bar{4}$.10.1	$\overline{13}$ 44	25 28
102	𝔣	1.6.10	6.10.1	9 06	35 34
103	*K*	$\bar{5}$.12.10	$\overline{12}$.10.5	$\overline{22}$ 18	54 08
104	*J*	213	132	60 48	40 49
105	χ	2.1.11	1.11.2	"	13 15
106	*i*	$\bar{2}$.1.10	$\bar{1}$.10.2	$\overline{64}$ 37	14 13
107	*β*	$\bar{2}36$	$\bar{3}62$	$\overline{33}$ 33	34 18
108	*T*	3.4.12	4.12.3	35 08	25 09
109	*ρ*	$\bar{4}13$	$\bar{1}34$	$\overline{77}$ 48	57 24
110	𝔟	$\bar{8}52$	$\bar{5}28$	$\overline{58}$ 53	79 17
111	*S*	$\bar{5}12$	$\bar{1}25$	$\overline{80}$ 41	70 45
112	λ	$\bar{3}$.2.18	$\bar{2}$.18.3	$\overline{57}$ 06	12 39
113	*δ*	324	243	53 57	46 22
114	*d*	$\bar{3}24$	$\bar{2}43$	$\overline{57}$ 06	45 17
115	Δ	$\bar{3}$.2.10	$\bar{2}$.10.3	"	22 00
116	𝔡	8.9.12	9.12.8	39 42	49 44
117	*e*	$\bar{5}24$	$\bar{2}45$	$\overline{69}$ 38	56 26
118	*H*	7.4.10	4.10.7	57 40	43 08
119	*o*	568	685	37 57	48 58
120	𝔤	328	283	53 20	27 43
121	Φ	$\bar{3}27$	$\bar{2}73$	$\overline{57}$ 06	29 20
122	𝔧	$\bar{6}47$	$\bar{4}76$	"	49 06
123	𝔨	315	153	58 51	36 02
124	𝔩	$\bar{3}74$	$\bar{7}43$	$\overline{22}$ 53	65 22
125	𝔷	728	287	71 21	46 14
126	𝔵	$\bar{3}57$	$\bar{5}73$	$\overline{30}$ 46	43 27
127	ℭ	524	245	65 21	57 15
128	𝔘	456	564	36 51	51 29
129	𝔇	345	453	35 07	49 41
130	𝔫	123	231	25 22	41 20

The gnomonic projecton on *b* (010), figure 40 shows the direction line of the base 2° 25′ to the right of the 90° coordinate. The positive pyramids are in the lower right hand, and upper left hand, quadrants. A crystal is brought from the normal to this position by two 90° rotations:

1. A 90° rotation from front to back—making the front pinacoid polar.
2. A second 90° rotation from right to left—bringing the side pinacoid of the *right* end of the crystal polar.

The forms which were positive in the first position will still be positive. It is important to note that if the pole of the side pinacoid of the left end of the crystal is brought to the center of the projection, the direction line of the base will be on the left of the 90° coordinate. The position of the positive and negative pyramids is also reversed, i. e. the negative forms will lie in the lower, right quadrant. Therefore, if the right end of a crystal is measured in the side pinacoid position, the ϕ of the base will be +87° 35′ and the ϕ values of the other forms will agree, in sign, with the table. If the left end is measured, the base will have a ϕ value of −87° 35′. In this case the *sign* of all the ϕ angles must be reversed to conform to the orientation used in calculating the table.

THE ANGLES OF AZURITE FROM OTHER LOCALITIES

Azurite crystals from different localities were next studied to test the new calculated angles, and to determine, if possible, any actual variation in the angles of crystals from different localities. In the following tables the average measured angles, together with the calculated angles from this paper and the Winkeltabellen, are given for comparison. The relative weight to be accorded each form depends upon the number of measurements and quality of the reflection obtained from the face. Poor reflections are usually not included and the entries under the column marked "Signal" indicate:—E-excellent, G-good, F-fair, P-poor.

CHESSY, FRANCE. Three specimens from this locality were obtained for crystallographic study. Most of the crystals are of the pyramidal habit forming a sub-parallel group on malachite pseudomorphs. Six such crystals were measured, but the signals were so confused that it was impossible to use them in checking the calculations. One vug, however, contained undisturbed crystals elongated parallel to the *b* axis, and projecting into the cavity. Four of these crystals were measured, and gave good reflections.

AZURITE FROM CHESSY, FRANCE—MEASURED ON *b*(010)

Letter	Signal	Number of faces	ϕ Calculated Winkel-tabellen	ϕ Calculated This paper	ϕ Measur'd	ρ Calculated Winkel-tabellen	ρ Calculated This paper	ρ Measur'd
c	F	2	87° 36′	87° 35′	87° 39′	90° 00′	90° 00′	90° 00′
η	G	1	$\overline{33}$ 28	$\overline{33}$ 36	$\overline{33}$ 36	"	"	"
θ	E	1	$\overline{45}$ 09	$\overline{45}$ 15	$\overline{45}$ 12	"	"	"
v	G	1	$\overline{26}$ 13	$\overline{26}$ 17	$\overline{26}$ 07	"	"	"
a	G	1	0 00	0 00	0 06	"	"	90 08
m	G	1	0 00	0 00	0 00	49 39	49 27	49 24
h	E	1	25 18	25 22	25 27	53 02	52 51	52 50
x	G	2	$\overline{45}$ 09	$\overline{45}$ 15	$\overline{45}$ 18	58 02	57 52	57 47
d	G	2	$\overline{57}$ 01	$\overline{57}$ 06	$\overline{57}$ 05	45 24	45 17	45 18
R	F	2	$\overline{26}$ 13	$\overline{26}$ 17	$\overline{26}$ 14	32 42	32 33	32 34
f	G	2	87 36	87 35	87 35	48 40	48 33	48 34
p	E	2	87 36	87 35	87 36	29 27	29 30	29 30

The measured angles consistently agree more closely with the new calculations than with the corresponding values in the Winkeltabellen. The disagreement between the elements obtained from Chessy measurements and from other localities seems to depend on the quality of material available for the early studies, rather than upon any actual variation in angles.

BISBEE, ARIZONA. A very fine collection was available for study from this locality. Nine crystals were measured. Four of the most perfect were averaged to check the axial ratio.

AZURITE FROM BISBEE ARIZONA—MEASURED ON $b(010)$

Letter	Signal	Number of faces	φ Calculated Winkeltabellen	φ Calculated This paper	φ Measur'd	ρ Calculated Winkeltabellen	ρ Calculated This paper	ρ Measur'd
c	P	5	87° 36′	87° 35′	87° 42′	90° 00′	90° 00′	90° 00′
a	F	6	0 00	0 0	0 00	"	"	"
σ	P	4	42 50	42 54	42 58	"	"	"
θ	F	4	$\overline{45}$ 09	$\overline{45}$ 15	$\overline{45}$ 21	"	"	"
m	G	7	0 00	0 00	0 02	49 39	49 27	49 31
w	G	2	0 00	0 00	0 02	30 29	30 18	30 10
l	F	6	87 36	87 35	87 57	59 37	59 30	59 21
f	G	7	"	"	87 40	48 40	48 33	48 36
p	G	7	"	"	87 38	29 27	29 30	29 31
h	F	7	25 18	25 22	25 39	53 02	52 51	52 54
s	F	4	42 50	42 55	43 03	59 06	58 57	58 55
P	F	2	53 46	53 50	54 02	64 40	64 33	64 33
γ	G	3	42 50	42 55	42 54	39 52	39 42	39 44
k	G	5	$\overline{26}$ 13	$\overline{26}$ 17	$\overline{26}$ 18	52 08	51 56	51 55
x	F	4	$\overline{45}$ 09	$\overline{45}$ 15	$\overline{45}$ 08	58 02	57 52	57 50
d	F	6	$\overline{57}$ 01	$\overline{57}$ 06	$\overline{57}$ 00	45 24	45 17	45 20
e	G	7	$\overline{69}$ 34	$\overline{69}$ 38	$\overline{69}$ 40	56 35	56 26	56 27
R	G	8	$\overline{26}$ 13	$\overline{26}$ 17	$\overline{26}$ 15	32 42	32 33	32 33
u	F	1	$\overline{57}$ 01	$\overline{57}$ 06	$\overline{56}$ 55	65 47	63 40	63 55
ρ	G	4	$\overline{77}$ 46	$\overline{77}$ 48	$\overline{77}$ 35	57 10	57 24	57 02
𝔮	F*	4		42 55	43 03		73 15	73 23
𝔦	P*	3		$\overline{9}$ 13	$\overline{10}$ 20		41 25	40 46
𝔠	P*	2		$\overline{13}$ 44	$\overline{13}$ 07		25 28	24 10
ℜ	E*	1		87 35	87 33		56 28	56 35

* New forms

LAURIUM, GREECE. Two specimens with brilliant azurite projecting into the opening of a partially filled veinlet yielded crystals of exceptional brilliance. These crystals are comparable to the Tsumeb suite in perfection and the angular agreement is correspondingly close. Four crystals were measured and averaged.

AZURITE FROM LAURIUM, GREECE—MEASURED ON (010)

Letter	Signal	Number of faces	ϕ Calculated Winkel-tabellen	ϕ Calculated This paper	ϕ Measur'd	ρ Calculated Winkel-tabellen	ρ Calculated This paper	ρ Measur'd
c	G	6	87° 36′	87° 35′	87° 35′	90° 00′	90° 00′	90° 00′
a	E	8	00 00	0 00	0 01	90 00	90 00	89 59
σ	G	2	42 50	42 54	42 55	90 00	90 00	90 00
v	F	6	$\overline{26}$ 13	$\overline{26}$ 17	$\overline{26}$ 01	"	"	"
θ	F	7	$\overline{45}$ 09	$\overline{45}$ 15	$\overline{45}$ 15	"	"	"
n	P	4	$\overline{64}$ 32	$\overline{64}$ 37	$\overline{64}$ 37	"	"	"
D	F	1	$\overline{77}$ 45	$\overline{77}$ 48	$\overline{77}$ 35	"	"	"
ψ	F	1	$\overline{18}$ 03	$\overline{18}$ 06	$\overline{17}$ 53	"	"	"
$\overline{11}$.0.13	P	1		$\overline{50}$ 14	$\overline{49}$ 36	"	"	"
$\overline{4}$.0.11	P	2		$\overline{71}$ 33	$\overline{71}$ 37	"	"	"
A	F	1	$\overline{73}$ 07	$\overline{73}$ 11	$\overline{73}$ 11	"	"	"
$\overline{4}$.0.13	P	1		$\overline{73}$ 59	$\overline{74}$ 00	"	"	"
m	E	6	0 00	0 00	0 01	49 39	49 27	49 26
h	E	8	25 18	25 22	25 21	53 02	52 51	52 51
k	P	2	$\overline{26}$ 13	$\overline{26}$ 17	$\overline{26}$ 20	52 08	51 56	51 55
x	G	4	$\overline{45}$ 09	$\overline{45}$ 15	$\overline{45}$ 21	58 02	57 52	57 53
d	G	8	$\overline{57}$ 01	$\overline{57}$ 06	$\overline{57}$ 07	45 24	45 17	45 16
e	G	6	$\overline{69}$ 34	$\overline{69}$ 38	$\overline{69}$ 40	56 35	56 26	56 26
ρ	F	2	$\overline{77}$ 46	$\overline{77}$ 48	$\overline{77}$ 58	57 10	57 24	57 08
R	E	6	$\overline{26}$ 13	$\overline{26}$ 17	$\overline{26}$ 17	32 42	32 33	32 33
P	G	2	53 46	53 50	53 50	64 40	64 33	64 33
s	E	4	42 50	42 55	42 54	59 06	58 57	58 57
l	G	6	87 36	87 35	87 33	59 37	59 30	59 30
f	F	4	"	"	87 33	48 40	48 33	48 32
p	E	6	"	"	87 34	29 27	29 30	29 30
$\mathfrak{r}$*	Line	1		$\overline{30}$ 46	$\overline{32}$ ..		43 27	43 10
$\mathfrak{f}$*	G	1		9 06	9 04		35 54	35 56
$\mathfrak{u}$*	Dim	1		$\overline{18}$ 07	$\overline{17}$ 39		36 03	36 15
$\mathfrak{t}$*	"	1		68 51	68 06		36 02	37 05
$\mathfrak{z}$*	"			71 21	72 16		46 14	46 40

* New forms.

KELLY, NEW MEXICO. Eight crystals were measured. Each crystal had from 25 to 40 faces, and four yielded over 35 readings. Measurements of the three most perfect crystals are included in the average.

AZURITE FROM KELLY MINE, NEW MEXICO—MEASURED ON (010)

Letter	Signal	Number of faces	ϕ Calculated Winkel-tabellen	ϕ Calculated This paper	ϕ Measur'd	ρ Calculated Winkel-tabellen	ρ Calculated This paper	ρ Measur'd
c	F	4	87° 36′	87° 35′	87° 37′	90° 00′	90° 00′	90° 00′
a	G	3	0 00	0 00	0 00	"	"	"
σ	F	2	42 50	42 54	42 53	"	"	90 02
v	P	2	$\bar{2}$6 13	$\bar{2}$6 17	$\bar{2}$6 45	"	"	90 00
η	P	2	$\bar{3}$3 28	$\bar{3}$3 36	$\bar{3}$3 28	"	"	"
θ	E	4	$\bar{4}$5 09	$\bar{4}$5 15	$\bar{4}$5 15	"	"	"
n	P	2	$\bar{6}$4 32	$\bar{6}$4 38	$\bar{6}$4 37	"	"	"
$\overline{11}$.0.13	F	2		$\overline{50}$ 14	$\bar{4}$9 32	"	"	"
α	P	1	$\bar{6}$9 34	$\bar{6}$9 38	$\bar{7}$0 11	"	"	"
$\bar{3}$.0.10	F	1		$\bar{7}$5 00	$\bar{7}$5 06	"	"	"
$\bar{5}$.0.3	Line	1		$\bar{3}$0 45	$\bar{3}$1 48	"	"	"
T	P	1	$\bar{5}$1 47	$\bar{5}$1 53	$\bar{5}$3 25	"	"	"
$\bar{4}$.0.13	P	1		$\bar{7}$3 59	$\bar{7}$4 03	"	"	"
A	F	1	$\bar{7}$3 07	$\bar{7}$3 11	$\bar{7}$3 09	"	"	"
F	P	1	$\bar{7}$5 44	$\bar{7}$5 48	$\bar{7}$6 02	"	"	"
m	E	6	0 00	0 00	0 01	49 39	49 27	49 26
w	E	4	0 00	0 00	0 02	30 29	30 18	30 18
l	F	3	87 36	87 35	87 39	59 37	59 30	59 31
f	F	4	"	"	87 39	48 40	48 33	48 35
p	G	5	"	"	87 33	29 27	29 30	29 32
h	E	6	25 18	25 22	25 25	53 02	52 51	52 51
s	P	3	42 50	42 55	43 08	59 06	58 57	59 04
P	P	2	53 46	53 50	53 47	64 40	64 33	64 35
γ	G	4	42 50	42 55	43 01	39 52	39 42	39 42
ω	E	5	25 18	25 22	25 24	33 36	33 25	33 26
ρ	G	5	$\bar{7}$7 46	$\bar{7}$7 48	$\bar{7}$7 43	57 10	57 24	57 02
d	G	4	$\bar{5}$7 01	$\bar{5}$7 06	$\bar{5}$7 07	45 24	45 17	45 16
e	F	5	$\bar{6}$9 34	$\bar{6}$9 38	$\bar{6}$9 52	56 35	56 26	56 24
R	F	3	$\bar{2}$6 13	$\bar{2}$6 17	$\bar{2}$6 07	32 42	32 33	32 36
δ	G	2	53 46	53 57	53 54	46 34	46 22	46 25
u	G	1	$\bar{5}$7 01	$\bar{5}$7 06	$\bar{5}$7 05	65 47	63 40	63 37
𝔮*	G	2		42 55	42 48		73 15	73 22
𝔣*	F	1		9 06	9 11		35 34	35 53
𝔠*	F	3		$\bar{1}$3 44	$\bar{1}$3 35		25 28	25 30
𝔪*	G	4		$\bar{4}$5 15	$\bar{4}$5 12		75 55	75 56
𝔩*	P	3		$\bar{2}$2 53	$\bar{2}$2 50		65 22	65 15
𝔧*	P	1		$\bar{5}$7 06	$\bar{5}$7 08		49 06	49 34
𝔥*	P	1		$\bar{5}$7 06	$\bar{5}$7 08		29 20	30 20

* New forms.

Broken Hill, New South Wales. A single crystal, in habit and brilliance very similar to the Tsumeb crystals, was measured. Although the following table includes only the average of two faces for each form, the excellent crystallographic quality justifies its inclusion to check the calculated angles.

Azurite from Broken Hill, N. S. W.—Measured on (010)

Letter	Signal	Notices	ϕ			ρ		
			Calculated		Measur'd	Calculated		Measur'd
			Winkel-tabellen	This paper		Winkel-tabellen	This paper	
c	G	2	87° 36′	87° 35′	87° 39′	90° 00′	90° 00′	90° 00′
a	E	1	0 00	0 00	0 02	"	"	"
σ	F	2	42 50	42 54	42 50	"	"	"
φ	P	1	25 18	25 22	25 56	"	"	"
η	G	2	$\bar{33}$ 28	$\bar{33}$ 36	$\bar{33}$ 35	"	"	"
θ	E	2	$\bar{45}$ 09	$\bar{45}$ 15	$\bar{45}$ 11	"	"	"
m	E	2	0 00	0 00	0 03	49 39	49 27	49 26
l	G	2	87 36	87 35	87 36	59 37	59 30	59 28
f	E	2	"	"	87 37	48 40	48 33	48 31
p	E	2	"	"	87 37	29 27	29 30	29 29
h	G	2	25 18	25 22	25 23	53 02	52 51	52 49
s	G	2	42 50	42 55	42 56	59 06	58 57	58 57
γ	G	2	42 50	42 55	43 08	39 52	39 42	39 48
k	F	2	$\bar{26}$ 13	$\bar{26}$ 17	$\bar{26}$ 12	52 08	51 56	51 55
R	F	2	$\bar{26}$ 13	$\bar{26}$ 17	$\bar{26}$ 17	32 42	32 33	32 30

Copiapó, Chile. Very small, needle-like crystals are clustered as a drusy coating on a specimen from this locality. The small size of the faces necessitates the use of the high-power magnifying lens in measurement. The signals are single and definite, and although the results are not quite as accurate as measurements on larger crystals, the following table can safely be interpreted as indicating that measured angles from this locality also are in close agreement with the new calculations.

AZURITE FROM COPIAPÓ, CHILE—MEASURED ON (010)

Letter	Signal	Number of faces	ϕ Calculated Winkel-tabellen	ϕ Calculated This paper	ϕ Measur'd	ρ Calculated Winkel-tabellen	ρ Calculated This paper	ρ Measur'd
c	G	2	87° 36′	87° 35′	87° 26′	90° 00′	90° 00′	90° 00′
a	F	2	0 00	0 00	0 00	"	"	"
σ	Line	1	42 50	42 54	42 22	"	"	"
v	"	1	$\bar{2}6$ 13	$\bar{2}6$ 17	$\bar{2}6$ 18			
θ	F	1	$\bar{4}5$ 09	$\bar{4}5$ 15	$\bar{4}5$ 26			
l	G	2	87 36	87 35	87 21	59 37	59 30	59 29
m	G	2	0 00	0 00	0 00	49 39	49 27	49 27
h	G	2	25 18	25 22	25 13	53 02	52 51	52 52
s	F	2	42 50	42 55	43 03	59 06	58 57	58 57
P	P	1	53 46	53 50	54 09	64 40	64 33	64 46
R	G	1	$\bar{2}6$ 13	$\bar{2}6$ 17	$\bar{2}6$ 16	32 42	32 33	32 34

CONCLUSIONS CONCERNING THE AXIAL RATIO OF AZURITE

In 1891, Farrington[3] made the first crystallographic study of azurite from Arizona, and deduced the ratio: .85676:1:88603, $\beta=87° 36' 36''$. He says: "In the position adopted by Schrauf the vertical axis is given double the length of that in our position. Taking, therefore, one-half the value which he gives to *c*, his axial ratio is:

$$\grave{a}:\bar{b}:c=.85012:\grave{1}:.88054, \quad \beta=87° 36'$$

It will be seen that these ratios differ but little, the values for β being almost identical, while those for $\grave{a}$ and *c* agree to the third decimal place. The author's value for $\grave{a}$ is supported by several very accurate measurements of the prism $m \wedge m$, which in every case showed a close approximation to the angle 81° 8′ instead of 80° 42′ as given by Schrauf. Whether this variation is to be regarded as a fundamental difference in the prismatic angle of the crystals from the separate localities or, on the other hand, as so small as to be within the limits of error in observation, I cannot say. More data are needed for deciding the question. The most satisfactory measurements that could be obtained for judging of the correctness of the value assigned to *c*, were those of $c \wedge p$,

[3] C. C. Farrington, *Am. J. Sc.*, Vol. **XLI**, April, 1891.

001∧021, and $p \wedge p$, 021∧02$\bar{1}$. The measured and calculated angles compare as follows:

	Calculated		Measured	
	Farrington	Schrauf	No. 1	No. 2
$c \wedge p$ 001∧021	60° 33′	60° 24′	60° 29′	60° 30′
$p \wedge p$ 021∧02$\bar{1}$	58 56	59 12	59 1	59 6

From these it would seem that the true value of *c* is about a mean between that given by Schrauf and by the author. Here, again, more accurate measurements are needed."

The value of *c*, as derived from the Tsumeb crystals, is .8844—a mean between the value assigned by Farrington and Schrauf.

The following table is taken from Farrington's paper with the addition of a column giving our calculated values for comparison.

Angles on the Orthopinacoid, *a*(100) and *a*($\bar{1}$00)—after Farrington

Letter	Symbol	Calculated			Crystal No. 1	Crystal No. 2	Other measurements
		Farrington	Schrauf	Palache & Lewis			
m	(110)	40° 34′	40° 21′	40° 33′	40° 34′	40° 33′	40° 30′
w	(120)	59 43	59 41	59 42			60 17
l	(023)	87 56	87 55.8	87 55		87 56	
f	(011)	88 12	88 12	88 11		88 16	
p	(021)	88 50	88 49	88 49	88 52	88 50	
σ	(101)	42 53	42 50	42 54	42 46	42 57	42 56
Q(*P*)	(223)	57 47	57 42	57 48	57 40	57 50	
h	(221)	43 56	43 45.5	43 56	43 50	43 58	
γ	(121)	62 7	61 58	62 7		62 12	
x	($\bar{1}$11)	53 22	53 15.5	53 24	53 31	53 18	
k	($\bar{2}$21)	45 5	44 55	45 6	45 19		
G	($\bar{3}$21)	33 35	33 26	33 36			33 30
K	($\bar{12}$.10.5)	39 48	39 37	39 48			39 55
F	($\bar{2}$07)	75 45	75 44	75 48	75 56		75 47
θ	($\bar{1}$01)	45 12	45 9	45 15	45 20	45 12	
η	($\bar{3}$02)	33 30	33 27.5	33 36			33 29

The measurements do not check closely with the calculated values, but the fact that our calculated angles agree so closely with Farrington's, shows that the variation is not to be regarded as "a fundamental difference in the prismatic angle from the separate localities." It has already been shown that measurements on sufficiently perfect azurite from Chessy agree more closely with our calculations than with Schrauf's. Our study on azurite from Bisbee, Laurium, Kelly, Broken Hill, and Copiapó indicates that the Tsumeb elements are in accord with measurements from these localities. The conclusion seems justified that the axial ratio of azurite is constant for these different localities, and that the new tables have a general, rather than local, value.

General Features of Azurite from Tsumeb

Most of the specimens selected for study had the azurite crystals implanted without mutual interference. The crystals elongated parallel to *c* are usually attached to the matrix at one end of the vertical axis. Those elongated parallel to the ortho axis are usually attached at one end of this axis. Many doubly terminated crystals are found delicately attached to the matrix or perched on needles of malachite. Symmetrical development is the rule. Small or thin crystals are transparent and of a beautiful azure blue color, while the thicker or larger ones are much darker. Prismatic development of the orthodome zone is the most common habit. These crystals usually have a wealth of forms developed with brilliant faces and sharp angles. Vicinal, etch, and line faces are rare. No twinned crystals were observed.

The larger crystals are commonly composed of parallel aggregates of several individuals. Often a malachite pseudomorph core is observed with second generation azurite in parallel or subparallel position.

The photographs reproduced in this paper were taken by Mr. E. B. Dane, Jr., a student at Harvard University. The reproduction of the colored photographs was made possible through the generosity of Mr. E. B. Dane, of Brookline, Mass. The authors welcome this opportunity to express their appreciation of the careful work necessary to obtain the detail found in the illustrations.

HABIT OF AZURITE FROM TSUMEB

In attempting to classify such a large number of crystals, the futility of strictly defining habit is apparent. The following classification is not exhaustive, but indicates the most important modifications observed.

Habit I. Elongated parallel to the *c* axis.

Type 1. Tabular parallel to *a* (100). Figure 1. Plate I, figure 2.
Dominant—*a* (100).
Prominent—*m* (110), *σ* (101).

" 2. Prismatic. Figure 3. Plate I, figures 4 and 5.
Dominant—*m* (110).

" 3. Elongated pyramidal. Plate I, figure 6.
Dominant—*h* (221), *m* (110).
Prominent—clinodome zone.

Habit II. Essentially equant parallel to *a*, *b*, and *c* axes.

Type 4. Dominant—*m* (110) and striated negative orthodome zone. Plate II, figures 7 and 8.

" 5. Dominant—*m* (110), *c* (001). Figures 10 and 11. Plate II, figure 9.

" 6. Dominant—*m* (110), *a* (100), *σ* (101), *θ* ($\bar{1}$01), *c* (001). Plate II, figure 12.

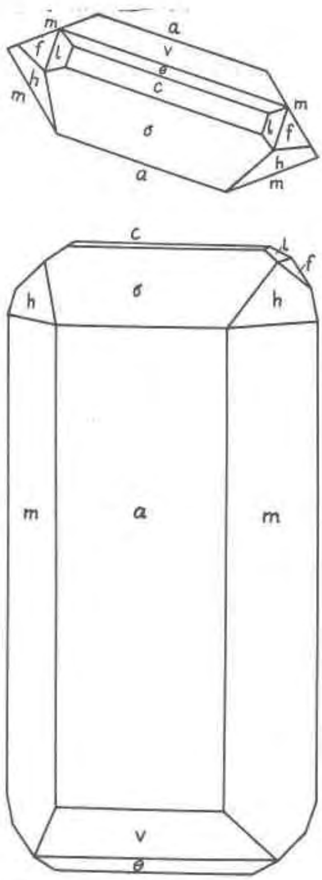

Fig. 1. Azurite. Projections, in Normal Position, of Crystal of Type 1.

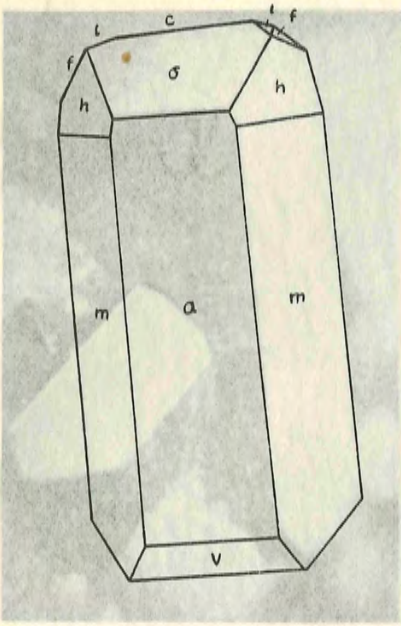

FIG. 2

Azurite of Type 1.

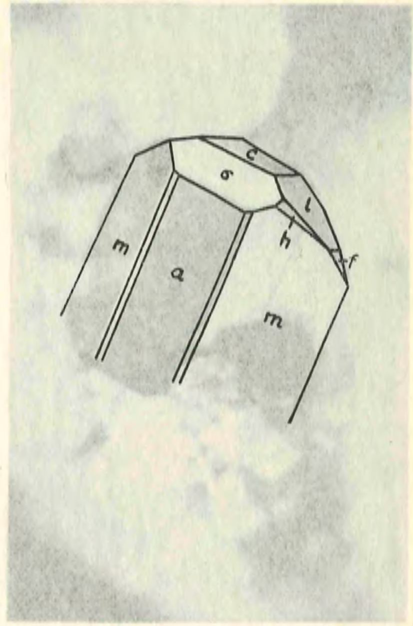

FIG. 4

Azurite Transitional between Types 1 and 2

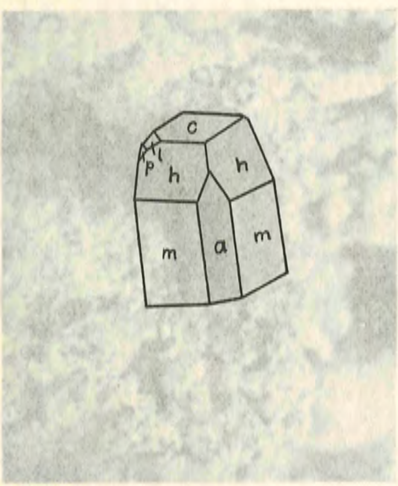

FIG. 5

Azurite Transitional between Types 2 and 3.

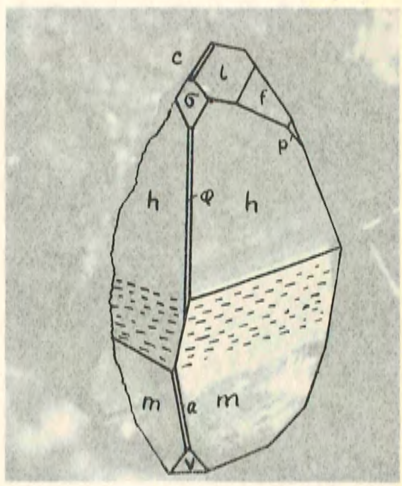

FIG. 6

Azurite of Type 3.

Plate I

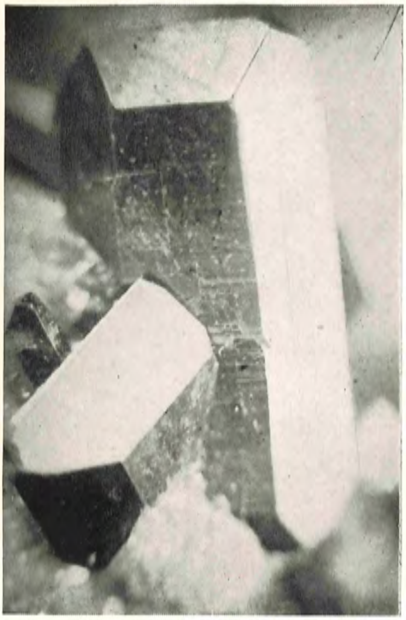

Fig. 2

Fig. 4

Fig. 5

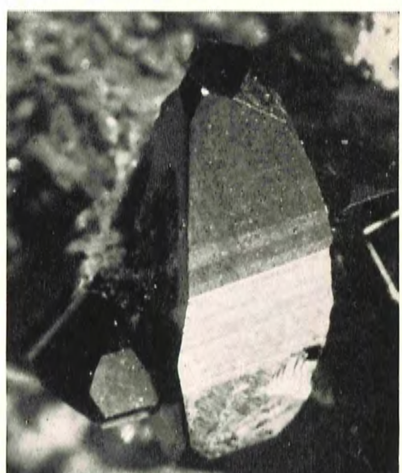

Fig. 6

PLATE II

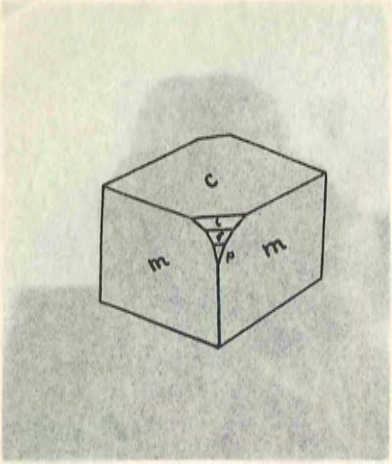

FIG. 7

Pseudo-rhombohedral Aspect of One Modification of Type 4.

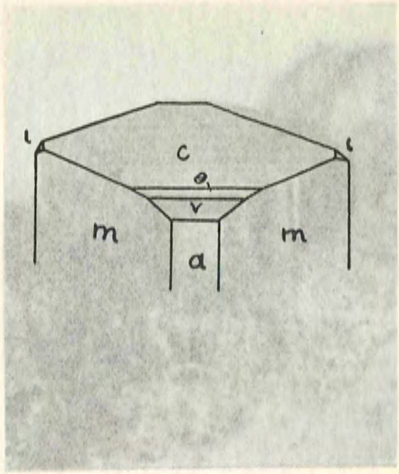

FIG. 8

Type 4. Simple Modification Dominated by Base and Prism.

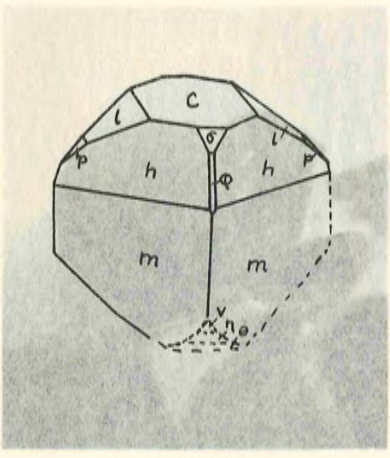

FIG. 9

Azurite of Pyramidal Habit.

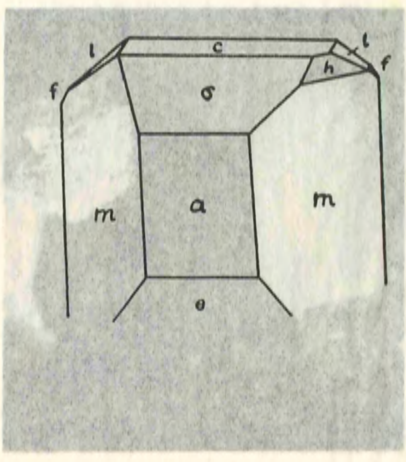

FIG. 12

Azurite of Type 6.

PLATE II

FIG. 7

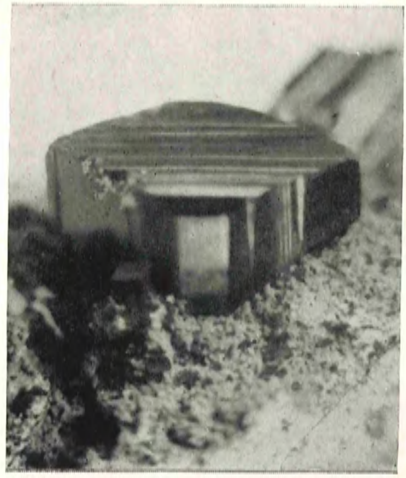

FIG. 8

FIG. 9

FIG. 12

Habit III. Elongated parallel to the *b* axis.

Type 7. Dominant in the orthodome zone—*a* (100). Figures 17 and 18. Plate III, figures 13, 14, 15, and 16.

" 8. Dominant in the orthodome zone—*c* (001). Figure 19. Plate IV, figures 20, 21, and 22.

" 9. Tabular parallel to striated negative orthodome zone approximating μ ($\bar{1}05$) in slope. Figures 23 and 24.

" 10. Plan of orthodome zone essentially equant. Figures 25 and 27. Plate IV, figure 26.

Habit IV. Tabular parallel to *c* (001).

Type 11. Dominant—*c* (001). Figure 28.

" 12. Dominant—*c* (001). Figure 30. Plate IV, figure 29.

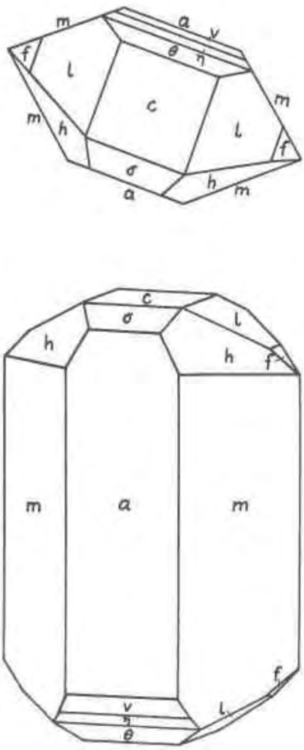

Fig. 3. Orthographic and Clinographic Projections of Azurite Crystal. Transitional between Types 1 and 2.

Habit I. Elongated parallel to the *c* axis.

Type 1. In this type the front pinacoid is dominant, and in the crystals examined *m* (110), *σ* (101), *v* ($\bar{2}$01), and *h* (221) are prominent. All the forms observed on this type are: *a* (100), *m* (110), *σ* (101), *v* ($\bar{2}$01), *θ* ($\bar{1}$01), *c* (001), *h* (221), *l* (023), *f* (011). Figure 1 shows the relative development of the forms. The crystals on specimen 87475 have a maximum size of 1.5×.8×.3 cm, and an individual crystal is illustrated in plate I, figure 2. Other specimens of this type are present in the collection, but no other forms were observed.

Type 2. The representative reproduced in plate I, figure 4, and figure 3 shows the forms: *m* (110), *a* (100), *c* (001), *σ* (101), *v* ($\bar{2}$01), *η* ($\bar{3}$02), *θ* ($\bar{1}$01), *l* (023), *f* (011), *h* (221), *s* (111). In the crystals studied, *a* (100), and *m* (110) dominate, and *c* (001), *l* (023), *σ* (101), and *θ* ($\bar{1}$01) are prominent. The crystal shown on plate I, figure 5, is transitional between types 2 and 3. The steep pyramid *h* (221) is well developed, but the truncation by the base prevents the elongation of type 3.

Type 3. The following list includes the most frequently occurring forms: *m* (110), *c* (001), *ϕ* (201), *σ* (101), *v* ($\bar{2}$01), *η* ($\bar{3}$02), *θ* ($\bar{1}$01), *l* (023), *f* (011), *p* (021), *h* (221). Other forms observed as small faces are: ($\bar{5}$03), *s* (111), *γ* (121), *P* (223), *k* ($\bar{2}$21), *R* ($\bar{2}$41), ($\bar{7}$71). The steep pyramid 𝔈 ($\bar{7}$71) has previously been reported from Tsumeb by Toborffy.[4] On one crystal measured it occurred as a line face between *R* ($\bar{2}$41) and *m* (110). The unit prism and pyramid *h* (221) are dominant, and the clinodome zone is prominent. The crystal shown on plate I, figure 6, is associated with divergent blades of malachite, and illustrates the zone of oscillation between pyramid and prism. Smaller azurite crystals less than 2 mm. in size are implanted on the malachite. Several large specimens in the collection have a steep slope due to the oscillation between *h* and *m*. Large sub-parallel aggregates are also common.

Habit II. Essentially equant parallel to the *a*, *b*, and *c* axes.

Type 4. Only five crystals of this type were observed. Plate II, figure 7, illustrates the pseudo-rhombohedral character resulting from the equal development of *m* (110) and the striated negative orthodome zone. The clinodome zone is prominent. The crystal shown on plate II, figure 8 is dominated by *m* and *c*.

Type 5. Symmetrical representatives are common in the collection. The equant habit of the crystal shown on plate II, figure 9 results from the approximation of the prism angle to a right angle, and the truncation of *h* by the base. Figure 10 shows the dominance of *m* and *c* and the prominent development of *h* (221), *P* (223), *β* ($\bar{3}$62), and the clino and orthodome zones. Figure 11 shows a different modification. The following list includes the forms observed on crystals of this type: *m* (110), *a* (100), *σ* (101), *ϕ* (201), *θ* ($\bar{1}$01), *v* ($\bar{2}$01), *η* ($\bar{3}$02), *c* (001), *l* (023), *f* (011), *p* (021), *h* (221), *P* (223), *k* ($\bar{2}$21), *e* ($\bar{2}$45), *β* ($\bar{3}$62). Farrington describes crystals of "Pyramidal Habit" corresponding to our crystals of types 3 and 5. He says, "Aside from the one just mentioned (Chessy) and a crystal from Cornwall figured by Zippe, I have found no other figures of azurite where the pyramid *h* predominates. This habit therefore may be considered peculiar to the Arizona azurites."

[4] Toborffy, *Zeit. Kryst.*, **1913,** 52.

PLATE III

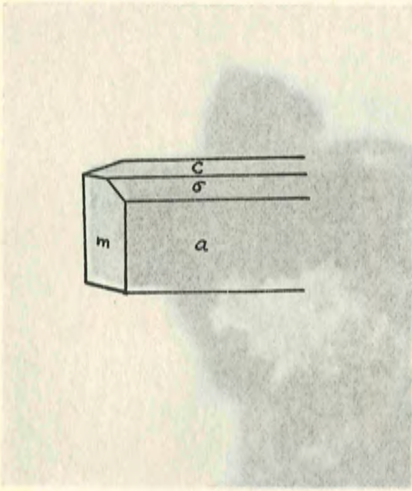

FIG. 13

Azurite of Type 7 with Few Forms.

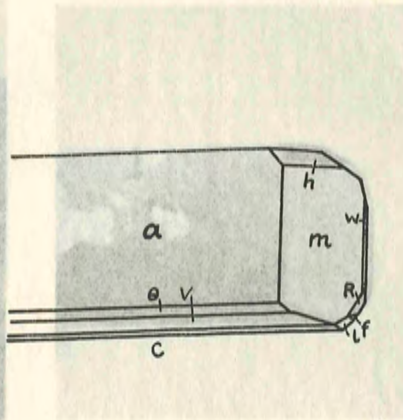

FIG. 15

Azurite of Type 7 with Complex Terminations.

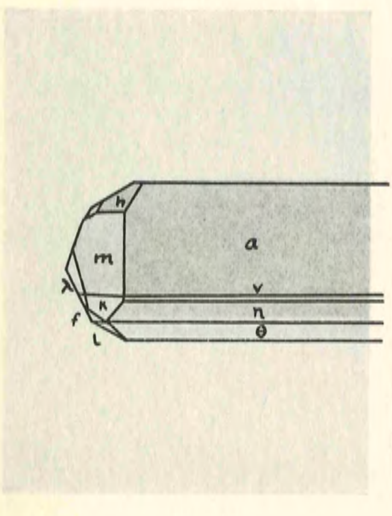

FIG. 16

Type 7. Terminations Dominated by Unit Prism

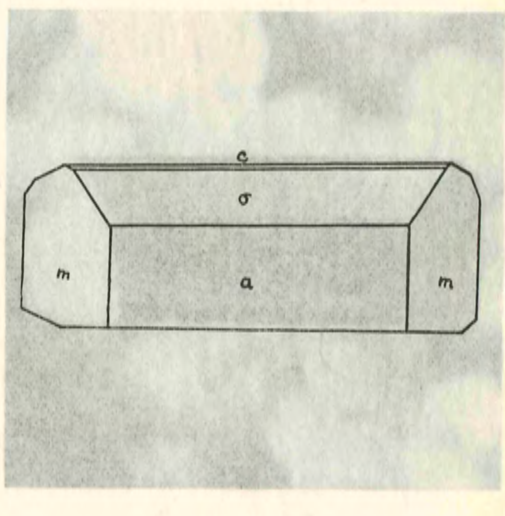

FIG. 14

Doubly Terminated Crystal of Type 7.

PLATE III

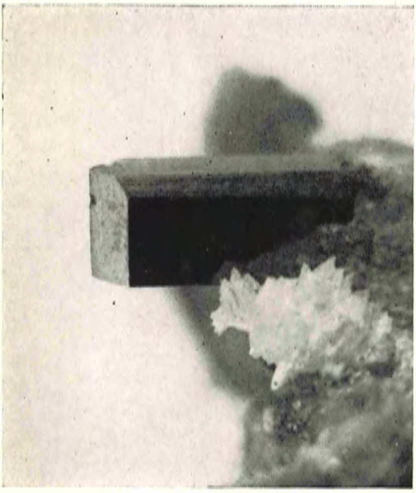

FIG. 13

FIG. 15

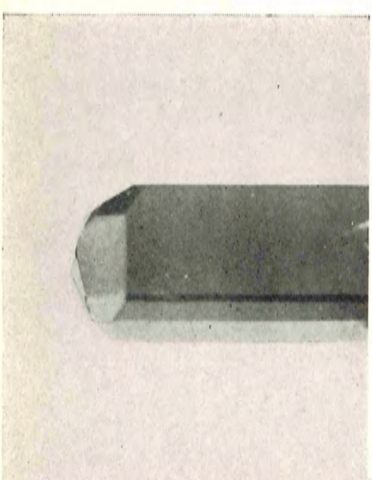

FIG. 16

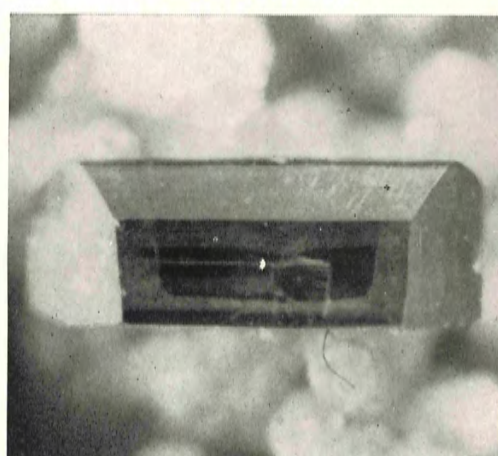

FIG. 14

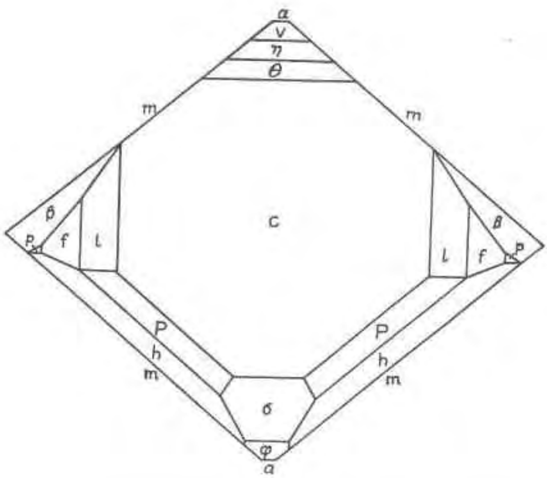

Fig. 10. Orthographic Projection of a Crystal of Type 5.

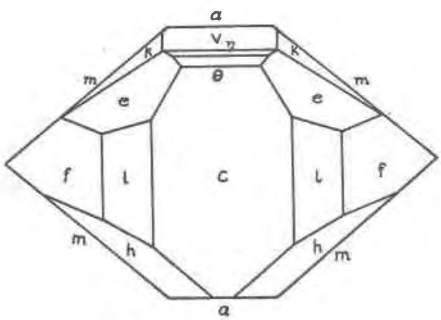

Fig. 11. Orthographic Projection of a Crystal of Type 5 with Enlarged Clinodomes and Negative Pyramids.

Type 6. Plate II, figure 12 illustrates this type in which the front pinacoid is surrounded by a ring of well developed faces. The forms *a* (100), *m* (110), *σ* (101), *θ* ($\bar{1}01$), and *c* (001) are dominant, and *l* (023), *f* (011), and *h* (221) are prominent.

Habit III. Elongated parallel to the *b* axis.

Type 7. These crystals are elongated parallel to the *b* axis and flattened parallel to the front pinacoid. Many are tabular parallel to the front pinacoid, but crystals in which it is the most prominent face in the orthodome zone are included. The collection contains many excellent representatives and plate III, figures 13, 14, 15 and 16, together with figures 17 and 18 illustrate the important modifications. The unit prism is the dominant truncation, but often the truncating forms are numerous. The forms observed are: *a* (100), *c* (001), *σ* (101), *θ* ($\bar{1}01$), *v* ($\bar{2}01$), *η* ($\bar{3}02$), *m* (110), *w* (120), *l* (023), *f* (011), *p* (021), *h* (221), *P* (223), *R* ($\bar{2}41$).

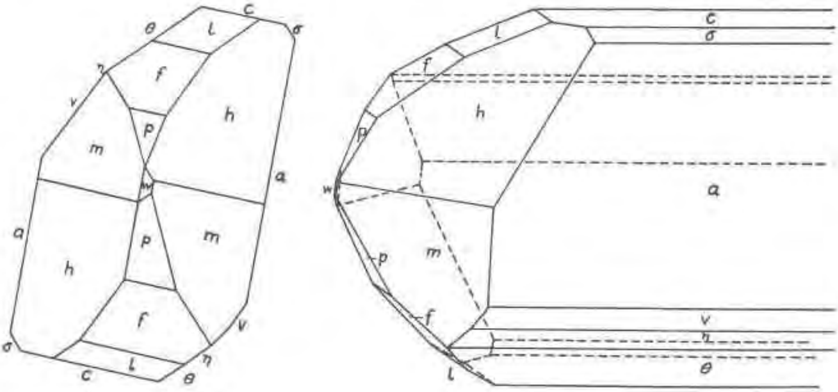

Fig. 17. Orthographic Projection on the Side Pinacoid, and Clinographic Projection in Normal Position, of Crystal of Azurite.

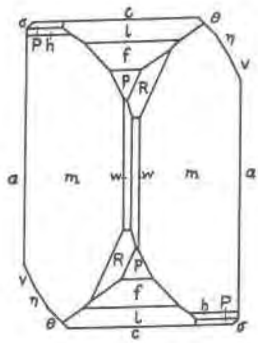

Fig. 18. Type 7. Orthographic Projection, on the Side Pinacoid, of Azurite Crystal Shown in Figure 16.

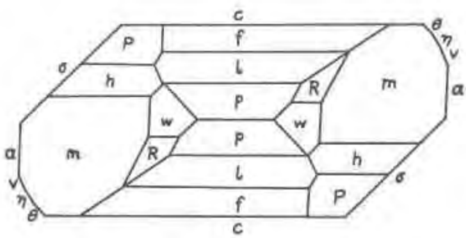

Fig. 19. Type 8. Orthographic Projection, on the Side Pinacoid, of Crystal Shown in Figure 20.

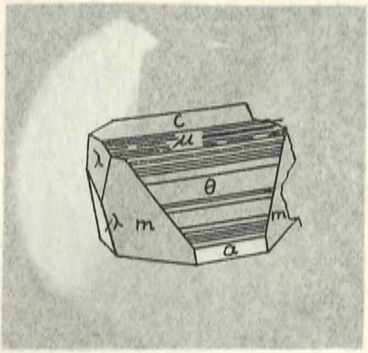

FIG. 21

Type 8. Dominated by λ.

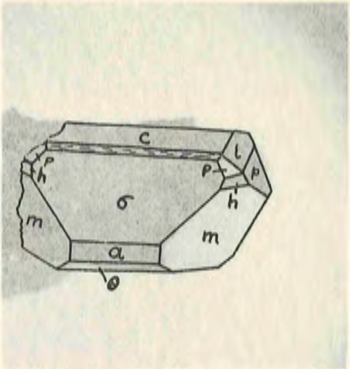

FIG. 20

Type 8. Clinodome Dominant.

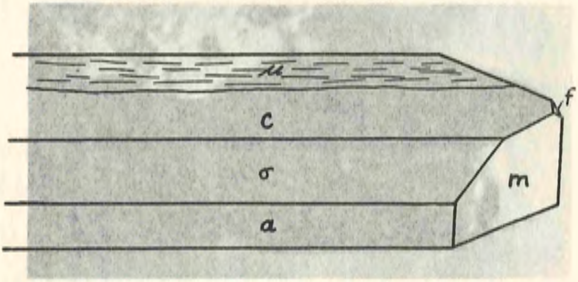

FIG. 22

Crystal tabular parallel to c and μ.

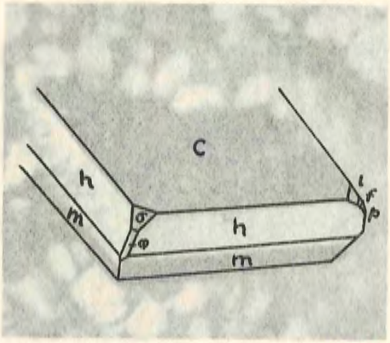

FIG. 29

Type 12. Compare with Figs. 5, 6 and 9.

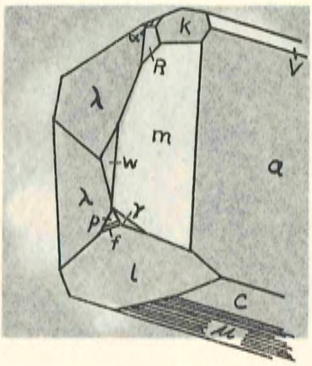

FIG. 26

Type 10. See Figure 25.

PLATE IV

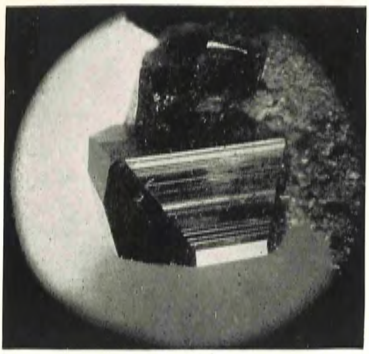

FIG. 21

FIG. 20

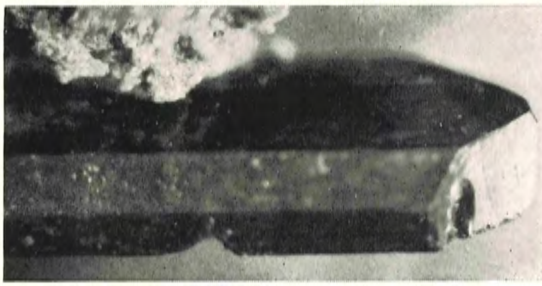

FIG. 22

FIG. 29

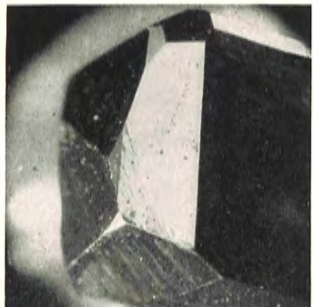

FIG. 26

Type 8. The crystals are elongated parallel to the *b* axis with *c* (001) dominant in the orthodome zone. Many of the crystals are tabular parallel to the base. Figure 19 is a plan of the crystal shown on plate IV, figure 20. In this modification *σ* (101) and *a* (100) are prominent in the orthodome zone, and *m* (110) and the clinodome zone are the prominent truncations. Plate IV, figure 21 shows a simpler modification with *m* (110) and λ ($\bar{2}$.18.3) the prominent truncations. Plate IV, figure 22 illustrates a mode flattened parallel to the base and truncated by the unit prism. The following forms were observed: *c* (001), *a* (100), *σ* (101), *θ* ($\bar{1}01$), *v* ($\bar{2}01$), *η* ($\bar{3}02$), *μ* ($\bar{1}05$), *m* (110), *w* (120), *l* (023), *f* (011), *p* (021), *h* (221), *P* (223), *R* ($\bar{2}41$), λ ($\bar{2}$.18.3)

Type 9. These crystals are tabular parallel to the negative striated orthodome zone. The resultant slope of this striated zone approximates *μ* ($\bar{1}05$) and is conspicuous for the small angle made with the base. In appearance this type is similar to the previous one, but the striations on the large face makes it easy to identify. The truncations are usually not complex and may be grouped as two modifications. One in which the unit prism is the dominant truncation and the other dominated by the flat pyramid λ ($\bar{2}$.18.3). Figure 23 illustrates a crystal with *m* as the dominant truncation. Figure 24 illustrates a modification in which the prism and clinodome form a frame for λ. The following forms were observed: *a* (100), *c* (001), *σ* (101), *θ* ($\bar{1}01$), *v* ($\bar{2}01$), *η* ($\bar{3}02$), *μ* ($\bar{1}05$), *m* (110), *l* (023), *p* (021), *d* ($\bar{2}43$), *e* ($\bar{2}45$).

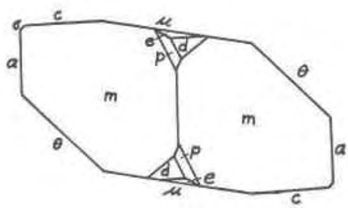

Fig. 23. Orthographic Projection, on the Side Pinacoid, of a Crystal of Type 9 with *m*(110) Dominant.

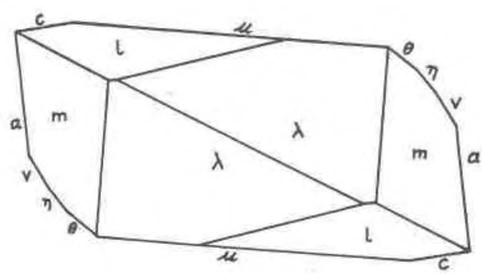

Fig. 24. Orthographic Projection, on the Side Pinacoid, of a Crystal of Type 9 with λ($\bar{2}$.18.11) Dominant.

Type 10. These crystals have a stocky appearance due to the equant plan of the orthodome zone. Figure 25 is drawn from a crystal from a large vug, and plate IV, figure 26 illustrates the terminations of another such crystal. The crystals are of desirable size for measurement, and faces unusually clean-cut and brilliant. Eight were measured and included in the average used in determining the axial ratio. Figure 25 shows the prominence of *m*, and λ as truncations. The zone of the three positive pyramids shown is typical and useful in orienting unmeasured crystals. The following forms were observed: *a* (100), *c* (001), σ (101), θ ($\bar{1}$01), *v* ($\bar{2}$01), η ($\bar{3}$02), μ ($\bar{1}$05), *l* (023), *f* (011), *p* (021), *m* (110), *w* (120), *h* (221), *s* (111), *P* (223), γ (121), *k* ($\bar{2}$21), *R* ($\bar{2}$41), α ($\bar{1}$21), λ ($\bar{2}$.18.3).

Figure 27 illustrates a modification in which the plan of the orthodome zone is similar to the one just described, but with λ as the only important termination. Crystals were observed in the collection where this pyramid was the only termination. The flat slope is very distinctive. In another modification λ is surrounded by a ring of narrow faces, as shown in figure 33. Forms observed on this mode are: *a* (100), *c* (001), σ (101), θ ($\bar{1}$01), *v* ($\bar{2}$01), η ($\bar{3}$02), c ($\bar{3}$.0.10), *F* ($\bar{2}$07), *l* (023), *p* (021), *m* (110), *h* (221), *d* ($\bar{2}$43), *e* ($\bar{2}$45).

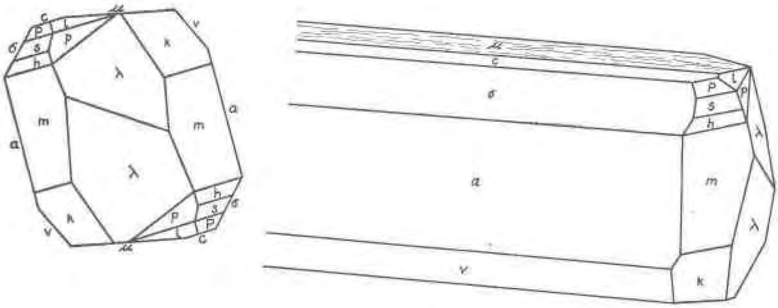

Fig. 25. Type 10. Orthographic Projection, on the Side Pinacoid, and Clinographic Projection in Normal Position, of Azurite Crystal. A very Common Habit.

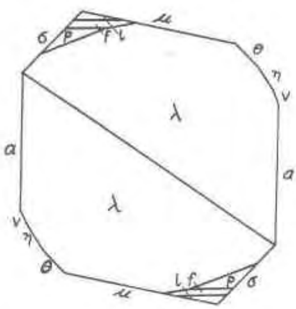

Fig. 27. Type 10. Orthographic Projection, on the Side Pinacoid, of a Crystal of Type 10.

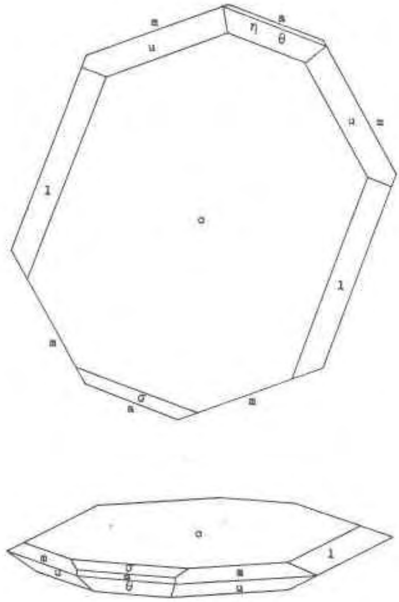

Fig. 28. Type 11. Orthographic and Clinographic Projections of a Crystal of Type 11.

Habit IV. Tabular parallel to *c* (001).

Type 11. The thin, platy crystals of this type were found on only three specimens. Figure 28 shows the development of forms. The clinodomes come to a sharp edge on the crystals from two specimens. On one the crystals have the side pinacoid present as a dull face, having more the appearance of being due to solution than to growth. This type is the only one on which the side pinacoid was observed. The equally developed ring of faces around the base is characteristic. The following forms were observed: *c* (001), *a* (100), *m* (110), σ (101), θ ($\bar{1}01$), η ($\bar{3}02$), *l* (023), *u* ($\bar{2}23$), *b* (010).

Type 12. These crystals are tabular parallel to the base, and the plan is dominated by the unit prism. Plate IV, figure 29, shows one of the crystals with *c* dominant, *m* and *h* prominent, and σ (101), ϕ (201), *l* (023), *f* (011), *p* (021) and λ ($\bar{2}$.18.3) present. Crystals with the modification illustrated in figure 30 are distinguished by the grouping of faces around the *b* axis. The forms observed are: *c* (001), *a* (100), σ (101), θ ($\bar{1}01$), η ($\bar{3}02$), *m* (110), *w* (120), *l* (023), *f* (011), *p* (021), *h* (221), *k* ($\bar{2}21$), *R* ($\bar{2}41$).

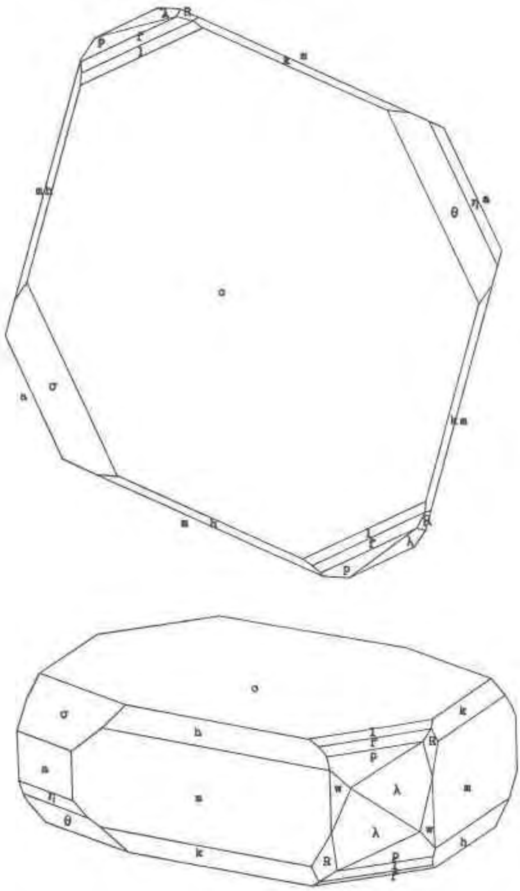

Fig. 30. Type 11. Orthographic and Clinographic Projections. The Clinographic Projection is Turned 20° from the *b* axis.

DISCUSSION OF FORMS OBSERVED ON TSUMEB AZURITE

A gnomonic projection, on the side pinacoid, of the forms observed on azurite from Tsumeb is reproduced in figure 40. The strong zonal relations are well shown. The poles of the common forms fall on important points in the network. The pyramid λ ($\bar{2}$.18.3) is an exception to this rule. The following table shows graphically the forms observed on each type together with the relative development of the form. The last column sums the number of types in which each form occurs.

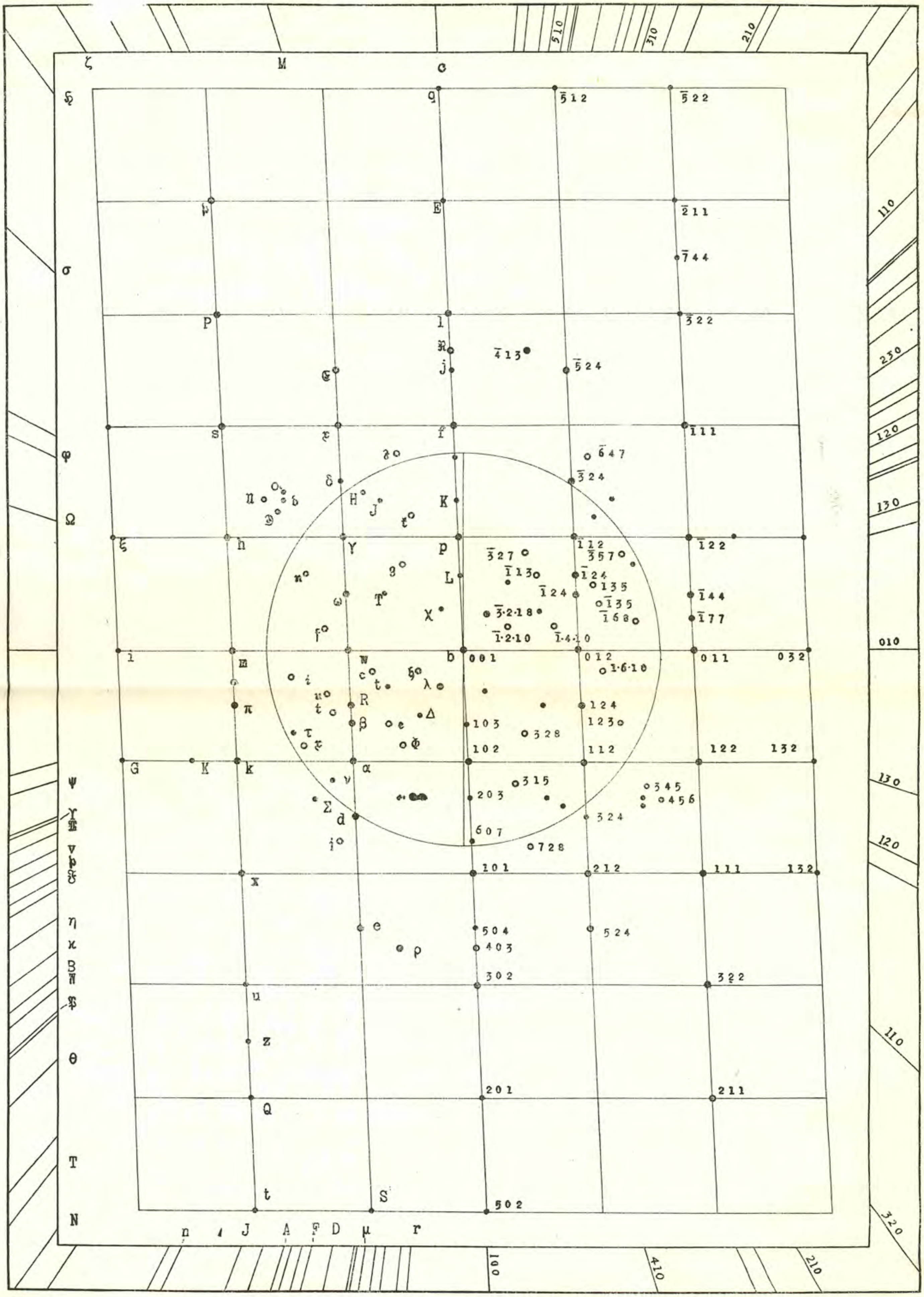

Figure 40. Gnomonic Projection on *b* (010), of all reported forms for Azurite.

○ New azurite forms. ● Forms observed on Tsumeb specimens. . Other reported forms

(See p. 101 for details of this projection.)

COMBINATION TABLE OF AZURITE FORMS FROM TSUMEB

Letter	Symbol (001)	Symbol (010)	Habit I			Habit II			Habit III				Habit IV		No. of types in which form occurs.
			Type 1	Type 2	Type 3	Type 4	Type 5	Type 6	Type 7	Type 8	Type 9	Type 10	Type 11	Type 12	
a	(100)	(010)	x	x			–	x	x	x	x	x	–	x	10
c	(001)	(100)	–	x	–	x	x	x	x	x	x	x	x	x	12
b	(010)	(001)											–		1
m	(110)	(011)	x	x	x	x	x	x	x	x	x	x	–	x	12
w	(120)	(012)							–	–		–		–	4
σ	(101)	(110)	x	x	–		–	x	–	x	–	x	–	x	11
φ	(201)	(120)			–		–							–	13
θ	$(\bar{1}01)$	$(\bar{1}10)$	–	–	–		–	x	–	–	–	–	–	–	11
v	$(\bar{2}01)$	$(\bar{1}20)$	x	–	–		–		–	–	–	–			8
η	$(\bar{3}02)$	$(\bar{2}30)$		–	–		–		–	–	–	–	–	–	8
μ	$(\bar{1}05)$	$(\bar{5}10)$									x	x			2
f	(011)	(101)	–	–	–	–	x	–	x	x		–		–	10
l	(023)	(302)	–	x	x	–	x	–	x	x	x	–	x	–	12
p	(021)	(102)			–	–	–		x	x	–	–		–	8
h	(221)	(122)	–	–	x		x	–	–	–		–		–	9
s	(111)	(111)		–	–							–			3
P	(223)	(322)			–		–		–	–		–			5
γ	(121)	(112)			–							–			2
k	$(\bar{2}21)$	$(\bar{1}22)$			–		–					–		–	4
α	$(\bar{1}21)$	$(\bar{1}12)$										–			1
R	$(\bar{2}41)$	$(\bar{1}24)$			–				–	–		–		–	5
e	$(\bar{2}45)$	$(\bar{5}24)$					x				–				2
d	$(\bar{2}43)$	$(\bar{3}24)$									–				1
u	$(\bar{2}23)$	$(\bar{3}22)$											x		1
β	$(\bar{3}62)$	$(\bar{2}36)$					–								1
λ	$(\bar{2}\cdot18\cdot3)$	$(\bar{3}\cdot2\cdot18)$								x	x	x		x	4

Legend:
x = Form present as a well developed face.
– = " " " " small face.

The numbers in the last column in the above table give a rough idea of the importance of the different forms.

c (001) was observed on every crystal examined. In habits tabular to it the base is present as a large square or rectangular face. In other cases it is usually present as a linear face. It is always brilliant but often gives double or multiple reflections.

m (110) was invariably present—usually with large faces. The signals normally yielded were single and strong and the angular variation found was slight.

w (120) is usually present as a small face on crystals of habit III. In crystals similar to the one shown in figure 18 it forms a long narrow truncation of the unit prism. It is more often present as a small triangle as illustrated in figure 19.

a (100) is usually present, either as a broad face or a long rectangle.

b (010) was only observed on one crystal, and then as a small, dull, line face. It may be considered an exceptional occurrence on azurite from Tsumeb. The recognition of the almost universal presence of the front and absence of side pinacoid is useful in orienting crystals for measurement.

σ (101) is nearly always present, although often as a small face. The face is brilliant and yields a good reflection.

ϕ (201) is the only other positive orthodome observed, and it is not common. It occurs usually as a long narrow face truncating the edge between the faces of *h* (221), and narrowing to a point upon meeting *a* (100) or *m* (110). See plate II, figure 9, and plate V, figure 29.

The negative orthodomes *θ* ($\bar{1}$01), *η* ($\bar{3}$02), *v* ($\bar{2}$01) usually occur together and in relatively equal development. Considering all the crystals observed the unit form is the best developed. Reference to the figures shows nearly all the crystals of habit III characterized by the presence of these three faces between the front pinacoid and base. The small angle between these faces is easily recognized.

The crystals of habit III usually have a striated negative orthodome face making a small angle with the base. This zone gives a long line of signals, and the signal corresponding to the average slope is that of *μ* ($\bar{1}$05). In drawing the crystals the pole of this face is used to represent this zone.

The clinodomes *l* (023), *f* (011), and *p* (021) are present on most of the types. The three faces usually occur together. *l* (023) was observed on all the types, *f* (011) on ten, and *p* (021) on eight. *l* (023) is ordinarily the largest face of the three. *p* (021) is characterized by its wedge shape due to the steep slope at which it bevels the other forms. See figures 5, 6, and 9.

The three positive pyramids *h* (221), *s* (111), and *P* (223) form a characteristic zone with base and unit prism in crystals of type 10. See figure 25.

h (221) is present on nine of the types and largely developed in two. The most striking crystals observed are of type 3 where it dominates, resulting in an extremely elongated habit parallel to the *c* axis. The face is always clean-cut and sharp and gives an excellent signal.

s (111), and *P* (223) are usually present as rectangular faces in zone with *h* (221).

γ(121) is not common and occurs only as a small face. See figure 26.

k ($\bar{2}$21) was observed on crystals of four types. The face is usually small, but gives a good reflection.

λ ($\bar{2}$.18.3) is commonly developed with large brilliant faces. It occurs in only four types, but a large proportion of the crystals in the collection belong to habit III, and the importance of this form is, therefore, greater than would be indicated by the table. It commonly is the largest truncating face, and occasionally is the only one present. See figures 21, 24, 25, 26, and 30. The signal given is excellent and undoubtedly the indices are correct.

R ($\bar{2}$41) is present as a small face on crystals of five types.

e ($\bar{2}$45) was observed on only two crystals. On the crystal illustrated in figure 11 it is present as a large striated face.

The negative pyramids *d* ($\bar{2}$43), *u* ($\bar{2}$23), *β*($\bar{3}$62) were observed only once as small faces.

PLATE V

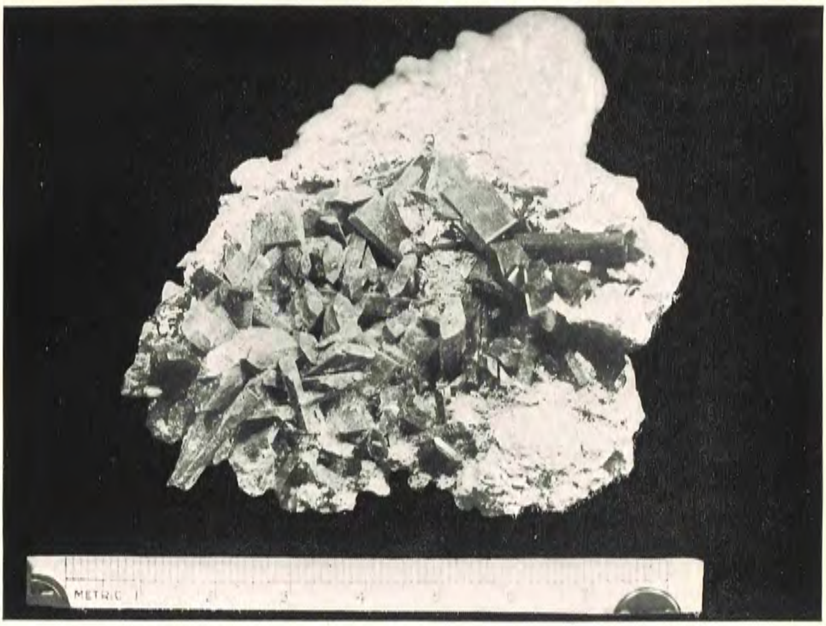

FIG. 31. Unaltered and Completely Altered Azurite in Contact.

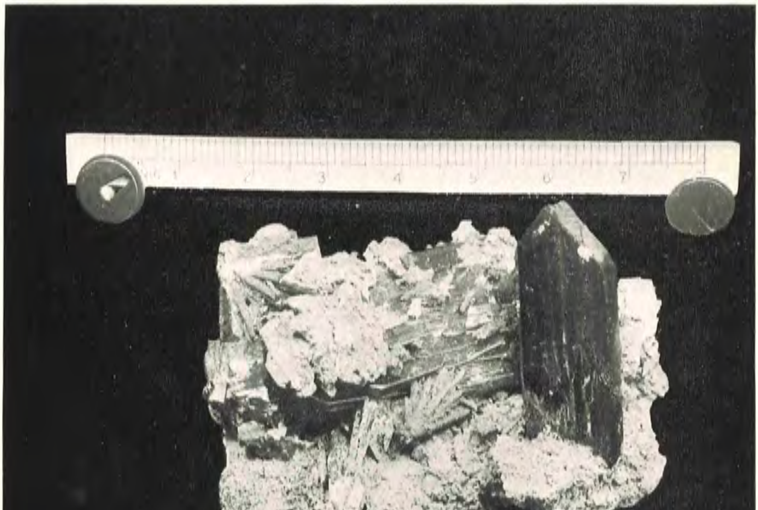

FIG. 32. Large Azurite Crystal of Type 8 with Bayldonite.

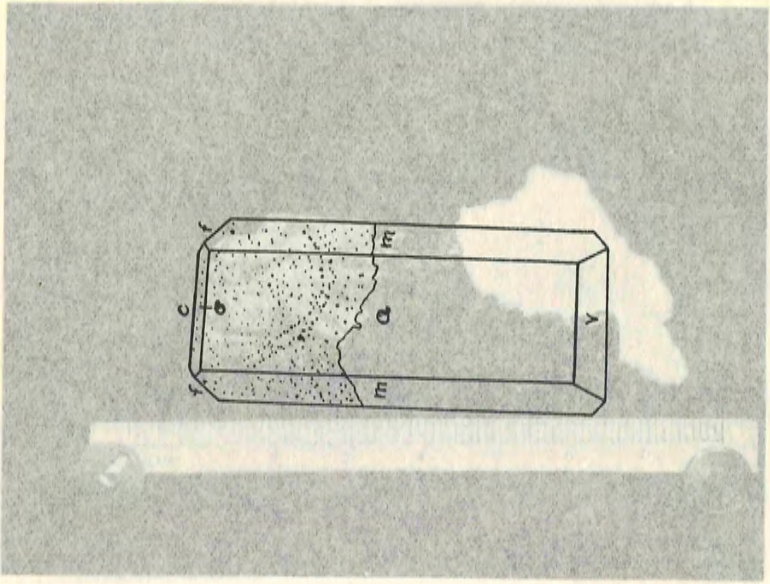

FIG. 34

Azurite Altering to Malachite

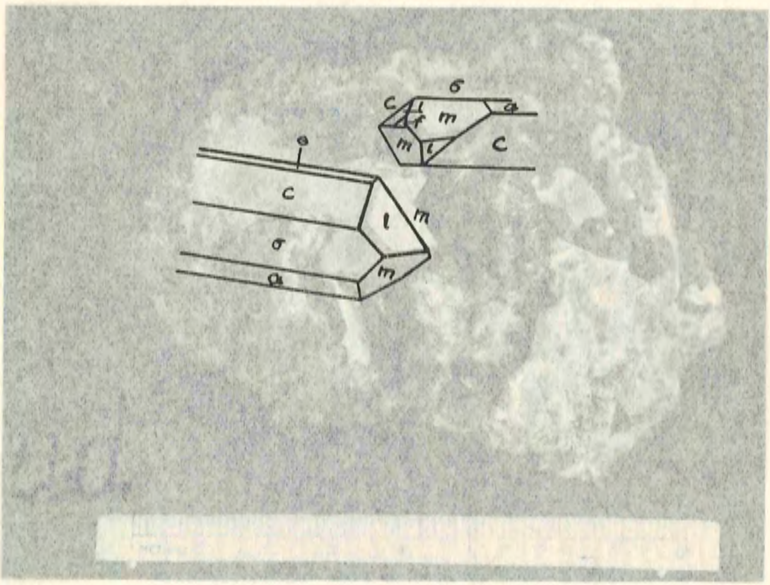

FIG. 35

Pseudomorph Group of Malachite after Azurite.

Plate VI

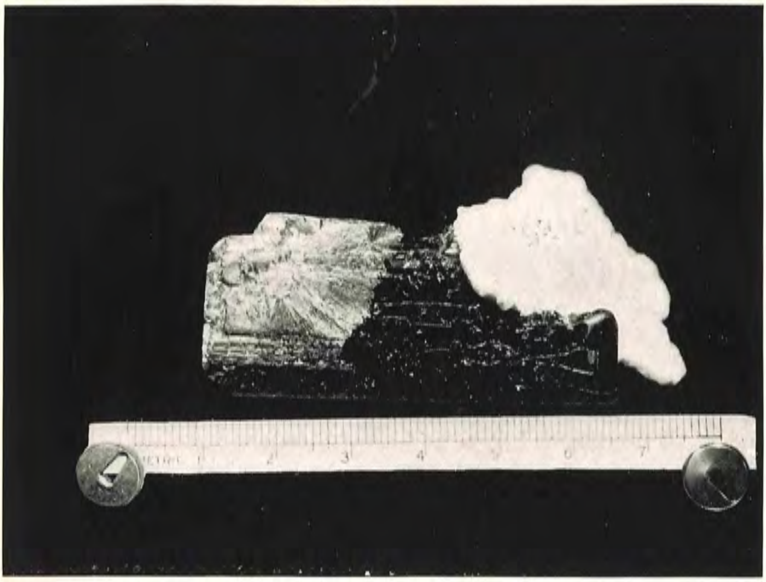

Fig. 34

Fig. 35

MALACHITE PSEUDOMORPHS AFTER AZURITE

Among the very numerous specimens in the collection of malachite pseudomorphs after azurite a large part retain their original outline so perfectly that the forms can be identified with certainty. On some hand specimens a single generation of azurite crystals has been partly changed to malachite with an abrupt boundary between the fresh and altered material. This condition is illustrated in plate V, figure 31. A few crystals of azurite on the right are unaltered and show absolutely no signs even of etching. All the other crystals have been replaced by malachite. The crystals are completely interlocking where attached to the matrix, and at the contact between azurite and malachite pseudomorphs, a few crystals are partially altered. The alteration has the appearance of starting at some center and progressively attacking fresh azurite, completely converting each crystal to malachite and spreading to the next at the point of contact.

Plate VI, figure 34, illustrates a partially altered crystal. The malachite fibers radiate from one important center on the front pinacoid, and many interfering centers on the prism, giving a confused network of interwoven, splendant fibers. The front of the invading malachite is roughly concentric normal to the fibers. Several darker colored bands in the malachite may be seen surrounding the center of radiation. In this specimen the contact is uneven with many individual malachite fibers penetrating beyond the common front.

The pseudomorph group shown on plate VI, figure 35, is attached to limestone containing a network of small veinlets of azurite and malachite. The drusy surface is covered with needlelike crystals of smithsonite, stained brown at the tips. The small size of the radiating group of malachite fibers can be dimly seen, but no picture could do justice to the delicate coloring and velvety texture.

The largest pseudomorph in the collection is shown on plate VII, figure 36. Several individuals in parallel position form the complete crystal, $10 \times 10 \times 5$ cm. in size, but the prism and pinacoid faces form practically a continuous surface. Comparison with plate VII, figure 37, illustrates the coarser, sheaf-like arrangement of the fibers.

The specimen from Bisbee illustrated on the frontispiece is a large malachite pseudomorph partially covered by parallel azurite crystals orientated to the original azurite axes. Similar examples were observed from Tsumeb. In some cases the azurite completely surrounds the malachite core. Figure 33 illustrates an example where the azurite wraps around the malachite pseudomorph without completely covering it. Apparently the pseudomorphs retain a structure adequate to control the orientation of later azurite deposited on their surface. The sequence of deposition of azurite, alteration to malachite, and later crystallization of azurite, indicates a delicate balance in the equilibrium relations.

The type of progressive alteration thus described for the figured specimens seems to be universal in the collection. A radiating fibrous or bladed structure of the invading malachite is the normal product of the change.

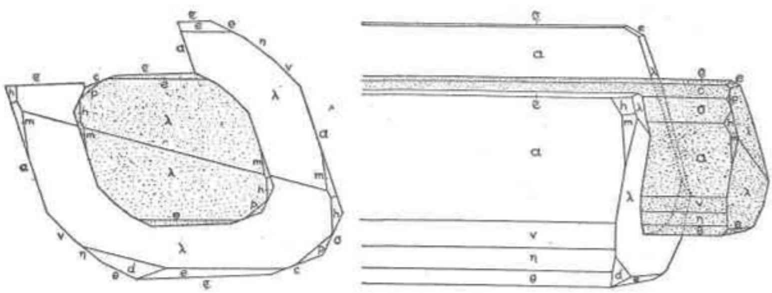

Fig. 33. Orthographic and Clinographic Projection of a Malachite Pseudomorph of Type 10 Partially Surrounded by a later Azurite Crystal in Parallel Position.

HABIT OF AZURITE FROM OTHER LOCALITIES AND FORMS OBSERVED

Azurite from Laurium, Greece

The crystals of the one specimen examined were elongated in the direction of the *b* axis, and tabular parallel to θ $(\bar{1}01)$. The habit is similar to that of crystals described by Zimányi[5] from this locality.

The following combination table shows the forms observed on the five crystals measured. (See figure 38.)

[5] K. Zimányi, *Zeit. Kryst.*, **21**, p. 86. 1882. The orthogonal projection shown in Fig. 22, Taf. V, of his paper illustrates the type observed on our crystals. This plan is reproduced in Goldschmidt's Atlas, Band V, Tafel 68, Figure 232

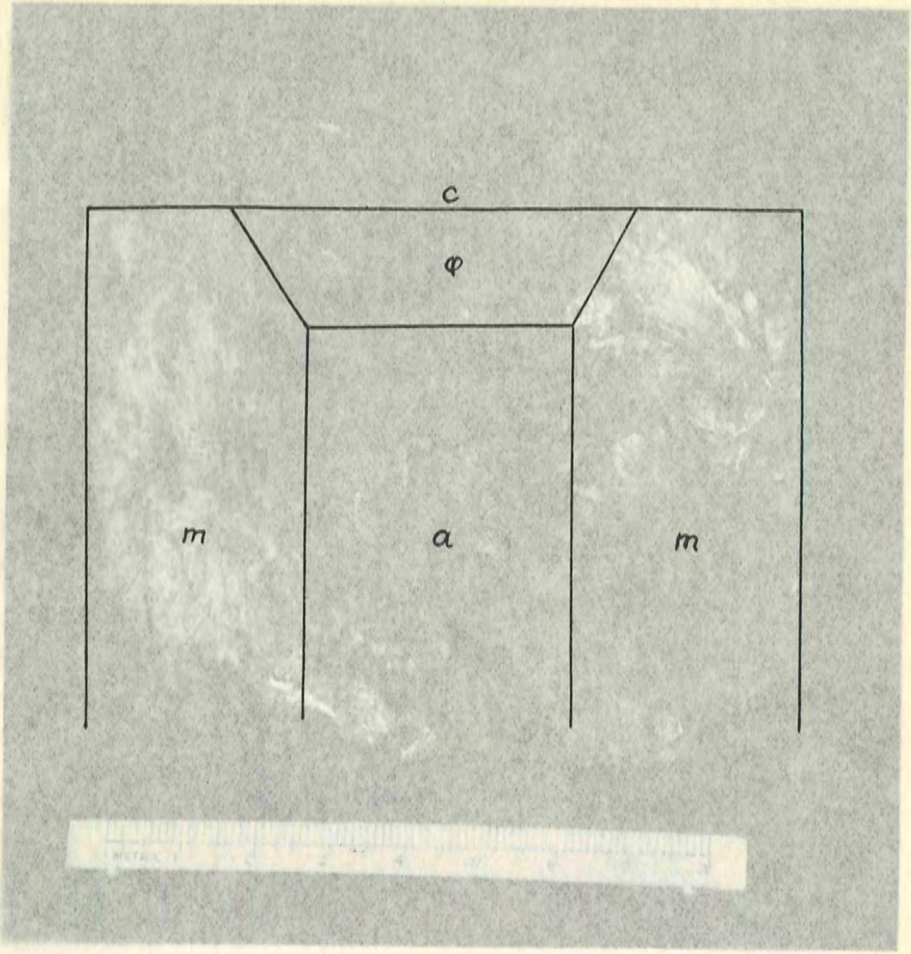

FIG. 36
Large Pseudomorph of Malachite after Azurite.

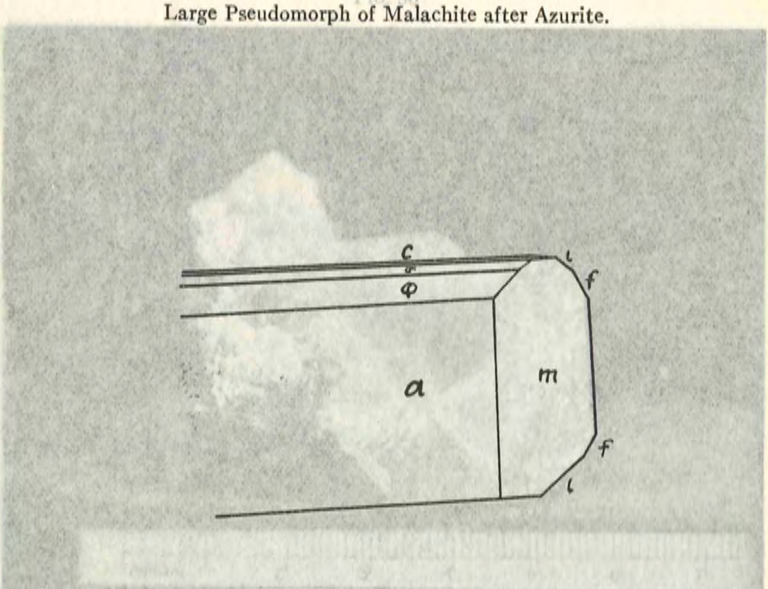

FIG. 37
Malachite Pseudomorph after Azurite.

FIG. 36

FIG. 37

Form	Number of crystal				
	1	2	3	4	5
c (001)	x	x	x	x	x
a (100)	x	x	x	x	x
σ (101)	x				x
v $(\bar{2}01)$	x	x	x	x	x
θ $(\bar{1}01)$	x	x	x	x	x
n $(\bar{1}02)$			x	x	x
D $(\bar{1}04)$				x	
$(\bar{7}.0.15)$		x		x	
ψ $(\bar{3}01)$				x	x
$(\bar{1}\bar{1}.0.13)$		x			
$(\bar{4}.0.11)$	x			x	
A $(\bar{1}03)$		x			
$(\bar{4}.0.13)$			x		
m (110)	x	x	x	x	x
h (221)	x	x	x	x	x
k $(\bar{2}21)$	x	x			x
x $(\bar{1}11)$		x	x	x	x
d $(\bar{2}43)$	x	x	x	x	x
e $(\bar{2}45)$	x	x	x	x	x
ρ $(\bar{1}34)$		x	x		x
R $(\bar{2}41)$	x		x	x	x
P (223)			x	x	x
s (111)	x		x	x	x
l (023)	x	x	x	x	x
f (011)	x	x	x	x	x
p (021)	x	x	x	x	x
ω (124)					x
*𝔣 (6.10.1)				x	x
*𝔯 $(\bar{3}.5.7)$ $(\bar{5}73)$				x	x
*𝔑 (564)					x
*𝔇 (453)					x
*𝔫 (123) (231)					x
*𝔲 $(\bar{1}35)$ $(\bar{3}51)$				x	
*𝔱 (315) (153)				x	
*𝔷 (728) (287)				x	
*Ω (301)					x

* New forms

The table on page 116 gives the average measured angles. New forms:

𝔣 (6.10.1) was observed on two crystals. It forms a triangular face between *m* (110) and *p* (021), and gives a sharp signal. It is also found on Kelly crystals.

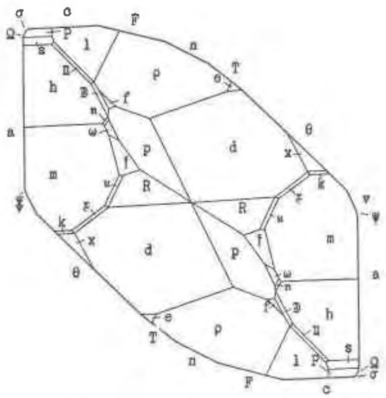

Fig. 38. Orthographic Projection, on the Side Pinacoid, of an Azurite Crystal from Laurium, Greece.

		ϕ	ρ
𝔣 (6.10.1)	Measured	9°03′	36°11′
		9 04	35 56
	Average	9 04	36 03
	Calculated	9 06	35 34
	Δ	0 02	0 29

𝔯 ($\bar{5}73$) is present on two crystals as a narrow line face between, and in zone with, *m* (110) and *d* ($\bar{2}43$). The signal was faint and difficult to center accurately.

		ϕ	ρ
𝔯 ($\bar{5}73$)	Measured	$\overline{32}$°—′	43°20′
		$\overline{31}$	43 10
	Average	$\overline{31}$ 30	43 15
	Calculated	$\overline{30}$ 46	43 27
	Δ	0 44	0 12

𝔑 (564) occurs as a line face between *l* (023) and *h* (221) and is in zone with them.

		ϕ	ρ
7 (564)	Measured	36°56′	51°48′
		37 —	51 18
	Average	37 —	51 33
	Calculated	36 51	51 29
	Δ	0 09	0 04

𝔇 (453) is also a line face and is in zone with *h* (221) and *f* (011).

		ϕ	ρ
𝔇 (453)	Measured	37°—′	49°30′
		36 —	49 24
	Average	36 30	49 27
	Calculated	35 07	49 41
	Δ	1 23	0 14

𝔫 (231) was observed as a narrow face between *h* (221) and *ω* (241), and it is definitely in zone with these two.

		ϕ	ρ
𝔫 (231)	Measured	24°48′	41°00′
		25 10	41 30
	Average	24 55	41 15
	Calculated	25 22	41 20
	Δ	0 27	0 05

𝔲 ($\bar{3}$51) was observed only once as a line face between *R* ($\bar{2}$41) and *m* (110).

	φ	ρ
Measured	17°39′	36°15′
Calculated	18 06	36 03
Δ	0 27	0 12

𝔱 (153) was only observed once.

	ϕ	ρ
Measured	68°06′	37°05′
Calculated	68 51	36 02
Δ	0 45	1 03

𝔷 (287). A line face between *h* (221) and *f* (011) gave a dim signal.

	ϕ	ρ
Measured	72°16′	46°40′
Calculated	72 21	46 14
Δ	0 55	0 26

Ω (301) was observed twice as a line face on crystal 5.

	ϕ	ρ
Measured	18°32′	90°00′
	19 00	90 00
Average	18 44	90 00
Calculated	17 39	90 00
Δ	1 05	0 00

Azurite from Kelly, New Mexico

The crystals studied from this locality are of four distinct types. The numbering will follow the scheme employed for the Tsumeb crystals to avoid confusion.

Habit I. Elongated parallel to the *c* axis.

Type 2. Prismatic.
Dominant—*m* (110).
Prominent—*a* (100), *c* (001), *σ* (101).

Type 3. Elongated pyramidal.
Dominant—*m* (110), *h* (221).
Prominent—*c* (001), *σ*·(110).

Habit III. Elongated parallel to the *b* axis.

Type 9. Tabular parallel to the negative orthodome zone.
Prominent in orthodome zone—*v* ($\bar{2}01$), *η* ($\bar{3}02$), *θ* ($\bar{1}01$), *n* ($\bar{1}02$), *a*(100), *c*(001).
Dominant truncation—*m* (110), *ρ* ($\bar{1}34$).
Prominent truncation—*h* (221), *d* ($\bar{2}43$).

Type 10. Plan of orthodome zone essentially equant.
Prominent in orthodome zone—*a* (100), *c* (001), *σ* (101).
Prominent truncations—*m* (110), *d* ($\bar{2}43$), clinodome zone.

The table on page 117 gives the average angles for the forms measured. The following combination table shows the forms observed on the different types.

Combination Table of Forms on Azurite from Kelly, N. M.

Letter	Miller Symbol (001)	Habit I			Habit III		
		Type 2	Type 3		Type 9		Type 10
		Crystal 1	2	3	4	5	6
c	(001)	x	x	x	x	x	x
a	(100)	x	x	x	x	x	x
b	(010)	x					x
σ	(101)	x	x	x	x		x
θ	($\bar{1}$01)	x	x	x	x	x	x
η	($\bar{3}$02)		x		x		x
v	($\bar{2}$01)		x	x	x	x	x
n	($\bar{1}$02)			x	x		
α	($\bar{2}$05)	x				x	
A	($\bar{1}$03)						x
ψ	($\bar{3}$01)		x				
F	($\bar{2}$07)		x				
T	($\bar{4}$05)				x		
	($\bar{5}$03)	x			x		
	($\bar{4}$.0.13)						x
	($\overline{11}$.0.13)					x	x
	($\bar{3}$.0.10)					x	
m	(110)	x		x	x	x	x
w	(210)	x		x		x	
l	(023)	x		x	x	x	x
f	(011)	x		x	x	x	x
p	(021)	x	x	x	x	x	x
h	(221)	x	x	x	x	x	x
s	(111)	x	x	x	x	x	x
P	(223)	x	x	x	x	x	x
γ	(121)		x	x	x	x	x
ω	(241)			x	x	x	x
k	($\bar{2}$21)			x	x	x	
ρ	($\bar{1}$34)	x	x		x	x	x
R	($\bar{2}$41)		x	x	x	x	x
d	($\bar{2}$43)	x	x	x	x	x	x
e	($\bar{2}$45)	x	x	x	x	x	x
u	($\bar{2}$23)			x		x	
$\mathfrak{p}$	(112)		x				
$\mathfrak{f}$	(6.10.1)			x			
$\mathfrak{j}$	($\bar{4}$76)			x			
$\mathfrak{h}$	($\bar{2}$73)			x			
$\mathfrak{l}$	(743)				x	x	
$\mathfrak{m}$	($\bar{5}$25)				x	x	
$\mathfrak{c}$	($\bar{4}$.10.1)					x	
$\mathfrak{q}$	(212)						x
δ	(243)		x		x	x	

New forms:

$\mathfrak{p}$ (112). This form was observed as a line face in zone between *c* (001) and *P* (223). The signal was not sharp but could be read to the nearest degree.

	ϕ	ρ
Measured	61° —′	69° —′
Calculated	60 48	68 54
Δ	0 12	0 06

$\mathfrak{f}$ (6.10.1) occurred on crystal 3 giving a poor but definite signal. This form was first observed on Laurium crystals.

Measured	9° 18′	35° 57′
Calculated	9 06	35 34
Δ	0 12	0 23

$\mathfrak{j}$ ($\bar{4}76$) also a line face giving a fair signal.

	ϕ	ρ
Measured	$\overline{57}$° 08′	49° 34′
Calculated	$\overline{57}$ 06	49 06
Δ	0 02	0 28

$\mathfrak{h}$ ($\bar{2}73$) was observed as a small face on crystal 3.

	ϕ	ρ
Measured	$\overline{57}$° 08′	30° 20′
Calculated	$\overline{57}$ 06	29 20
Δ	0 02	1 00

$\mathfrak{l}$ (743) is present as a large etch face on crystal 4. The signal was blurred but the second reading below was centered on a discernible signal.

	ϕ	ρ
Measured	23° 30′	65° —′
	23 09	65 26
	21 52	65 —
Average	22 50	65 08
Calculated	22 53	65 22
Δ	0 03	0 14

$\mathfrak{w}$ ($\bar{5}25$) forms well developed faces between *d* ($\bar{2}\bar{4}3$) and θ ($\bar{1}01$) on crystals 4 and 5. The signals were good.

	ϕ	ρ
Measured	$\overline{45}$° 12′	75° 53′
	$\overline{45}$ 14	76 00
	$\overline{45}$ 07	75 54
Average	$\overline{45}$ 12	75 56
Calculated	$\overline{45}$ 15	75 55
Δ	0 03	0 01

c ($\bar{4}$.10.1) was present on crystal 5 as a good face giving a fair signal. It was also observed on Bisbee crystals.

	ϕ	ρ
Measured	$\overline{13}$° 36′	25° 33′
Calculated	$\overline{13}$ 44	25 08
Δ	0 08	0 05

q (212) This form was present as two good faces on crystal 6, lying in zone between σ (101) and s (111). It is also present on Bisbee crystals.

	ϕ	ρ
Measured	42° 41′	78° 20′
	42 55	73 24
Average	42 48	73 22
Calculated	42 55	73 15
Δ	0 07	0 07

Azurite from Bisbee, Arizona

The crystals observed on six hand specimens studied belong to two types:

Habit III. Elongated parallel to the *b* axis.

Type 9. Flattened parallel to negative orthodome zone.

Prominent in orthodome zone—*v* ($\bar{2}$01), η ($\bar{3}$02), θ ($\bar{1}$01).

These crystals were taken from the deeper workings of the Copper Queen Mine in 1909 and reach a length of 5 cm. with greatest diameter of 2 cm. They are implanted as a secondary growth in parallel position upon well formed pseudomorphs of malachite after azurite of even larger dimensions, the largest pseudomorph having a length parallel to the *b* axis of 7 cm. These characteristics are illustrated in the specimen shown on the colored plate. The azurite crystals are of magnificent blue color on the exterior but for the most part, when broken through, a green malachite center is visible which indicates that the second generation of azurite is also in process of alteration to malachite. Some of the crystals present both terminations with reference to the *b* axis and the quality of the faces except in the orthodome zone, which is somewhat striated, is of the best.

Three crystals were measured and the presence of the following forms shown in figure 39 in average development, was established.

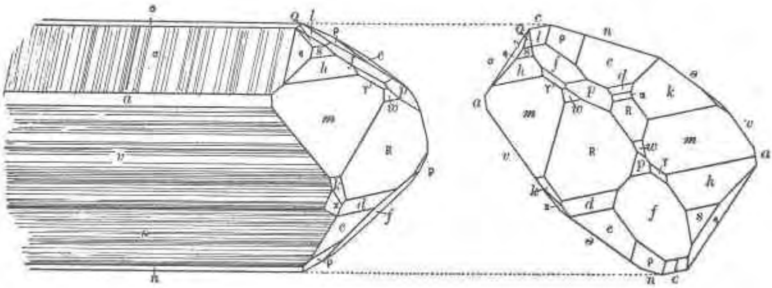

Fig. 39. Clinographic and Orthographic Projections, on the Side Pinacoid, of Azurite from Bisbee, Arizona.

c (001), *a* (100), *m* (110), *w* (120), *l* (023), *f* (011), *p* (021), *σ* (101), *μ* ($\bar{1}$05), *A* ($\bar{1}$03), *n* ($\bar{1}$02), *θ* ($\bar{1}$01), *h* (221), *s* (111), *P* (223), *k* ($\bar{2}$21), ꝗ (212), *R* ($\bar{2}$41), *ρ* ($\bar{1}$34), *d* ($\bar{2}$43), *e* ($\bar{2}$45), *γ* (121), *α* ($\bar{1}$21).

Habit V. Tabular parallel to *σ* (101).

Dominant—*σ* (101)

Prominent—*m* (110), *h* (221), *l* (023), *f* (010), p (021).

Crystals of this habit occur as reticulated plates on a specimen from the Czar mine. The following forms were identified: *c* (001), *a* (100), *σ* (101), *v* ($\bar{2}$01), *θ* ($\bar{1}$01), *m* (110), *l* (023), *f* (011), *p* (021), *h* (221), *P* (223), *k* ($\bar{2}$21), *R* ($\bar{2}$41), *e* ($\bar{2}$45).

New forms:

ꝗ (212). This form, which was also identified on the Kelly crystals, occurs as a large face between *σ* (101) and *f* (011).

	φ	ρ
Measured	43° 23′	73° 28′
	43 06	73 16
	42 53	73 31
	42 51	73 09
Average	42 33	73 23
Calculated	42 55	73 15
Δ	0 22	0 08

i ($\bar{6}$81) occurs as a line face between *R* ($\bar{2}$41) and *m* (110) and is in zone with them.

	φ	ρ
Measured	$\bar{9}$° 37′	41° 20′
	$\bar{1}$0 44	40 —
	$\bar{1}$0 44	40 30
Average	$\bar{1}$0 22	40 37
Calculated	$\bar{9}$ 13	41 25
Δ	1 09	0 48

c ($\bar{4}$.10.1) was identified on one crystal as a small face. It was first observed on Kelly specimens.

	ϕ	ρ
Measured	$\bar{1}\bar{3}$° 07′	24° 10′
Calculated	$\bar{1}\bar{3}$ 44	25 24
Δ	0 37	1 14

Azurite from Barnaul, Siberia

Etched azurite crystals associated with malachite coatings are found in cavities of a quartz vein. The crystals are elongated parallel to the orthodome zone and tabular parallel to *θ* ($\bar{1}01$).

Habit III. Elongated parallel to the *b* axis.
  Type 9. Tabular parallel to *θ* ($\bar{1}01$).
    Dominant in orthodome zone—*θ* ($\bar{1}01$).
    Prominent in orthodome zone—*a* (100) and *σ* (101).
    Prominent truncations—*m* (110), *h* (221), *p* (021).

The faces of the orthodome zone are only slightly etched but the truncating forms are badly pitted and it was often necessary to use alcohol to obtain a signal. The side pinacoid is always present as a rather large rectangular face.

Azurite from Copiapó, Chile

One hand specimen had small needle-like crystals of azurite forming a drusy coating. They are elongated parallel to the *b* axis and tabular parallel to the negative striated orthodome zone. The following forms were observed:

c (001), *a* (100), *σ* (101), *v* ($\bar{2}01$), *θ* ($\bar{1}01$), *m* (110), *l* (023), *p* (021), *h* (221), *s* (111), *R* ($\bar{2}41$), and *e* ($\bar{2}45$).

Azurite from Chessy, France

The crystals from this locality that were quite perfect and used to check the axial ratio are elongated parallel to the *b* axis and tabular parallel to the base.

Habit III. Elongated parallel to the *b* axis.
  Type 8. Tabular parallel to *c* (001).
    Dominant in the orthodome zone—*c* (001).
    Prominent in the orthodome zone—*v* (201), *θ* ($\bar{1}01$).
    Prominent truncations—*m* (110), *x* (111).

The front pinacoid is absent and the sharp angle between negative orthodomes and the base gives a thin wedge-like appearance. The following forms were also observed: *f* (011), *p* (021), *h* (221), *R* ($\bar{2}41$), *e* ($\bar{2}45$).